



# MONASH University

## **BACTERIA ENCAPSULATION USING SYNTHESIZED POLYUREA FOR SELF-HEALING OF CEMENT PASTE**

Mohammadhossein Zamani

Dr. Ahmad Mousa

Dr. Daniel Kong

Dr. Arash Behnia

A thesis submitted for the degree of Master at Monash University in 2019

School of Engineering

## **Copyright notice**

### **Notice 1**

© Mohammadhossein Zamani (2019).

## Abstract

Micro-cracks do not necessarily affect concrete strength, but they are more likely to intensify permeability and exacerbate the detrimental effects of chemicals and weathering. Most bio-treatment approaches that utilize bacteria have shown high potential to self-heal cementitious media by forming calcium carbonate. However, direct addition of bacteria and nutrition into a concrete mix have adverse effect on its properties. Additionally, the viability of bacteria needed for concrete self-healing decreases with time. This study proposed the use polyurea as a suitable polymeric carrier and shield for the bacteria. Polyurea was used to encapsulate the *bacillus pseudofirmus* bacteria and calcium lactate (nutrition) and subsequently utilized to self-heal artificially cracked cement paste specimens. Synthesis and encapsulation of the bacteria in the polyurea were performed using the in-situ polymerization method. The synthesized capsules have irregular shapes and rough surfaces, with 57% of the capsules ranging from 0.3 to 0.6 mm. FTIR results of the encapsulated polyurea capsule (EPU) showed that NCO peak (isocyanate group exist in polyurea) has completely disappeared, meanwhile urea bond N-H was observed. These observations indicate successful synthesis of the polyurea polymer structure and encapsulation of the bacterial spores. EDX analysis of the polyurea capsules and EPU showed the presence of calcium in EPU, which suggests successful encapsulation of calcium lactate. The observed calcium carbonate precipitation around the cracked zone of the cement paste specimens after 3 days proves self-healing triggered by EPU. The bacterial growth (from dormant to active) and calcium carbonate precipitation were confirmed via destructive and non-destructive testing. TGA and FTIR analysis showed precipitation of polymorph calcium carbonate. XRD analysis further confirmed that the crystal structure of the precipitated calcium carbonate is calcite. The polyurea has collectively proven to have the capacity to protect bacteria from harsh environment and to provide a prominent healing effect in cementitious materials. Polyurea equally possesses excellent and adaptable mechanical properties which are needed to shield (encapsulate) the bacteria used for healing.

## **Declaration**

This thesis contains no material which has been accepted for the award of any other degree or diploma at any university or equivalent institution and that, to the best of my knowledge and belief, this thesis contains no material previously published or written by another person, except where due reference is made in the text of the thesis.

Signature:

A large black rectangular redaction box covers the signature area. Above it is a thin, light-colored horizontal bar.

Print Name: MOHAMMADHOSSEIN ZAMANI

Date: 12/04/2019

## Table of Contents

1. INTRODUCTION .....	1
1.1 Background .....	1
1.2 Problem Statement .....	3
1.3 Objectives.....	3
1.4 Organization .....	4
2. LITERATURE REVIEW .....	6
2.1 Autogenous Self-Healing .....	6
2.2 Autonomous Self-Healing.....	8
2.2.1 Using capsules .....	8
2.2.2 Using vascular system.....	14
2.3 Biotechnology for Self-Healing .....	15
2.3.1 Bio-mineralization of bacteria .....	16
2.3.2 Biology basis.....	17
2.3.3 Self-healing using bacteria.....	17
2.3.4 Challenges.....	20
2.4 Summary of Self-Healing Attempts.....	21
2.5 A New Class of Material for Protection of Bacteria .....	23
3. RESEARCH METHODOLOGY .....	26
3.1 Materials.....	26
3.1.1 Bacterial strain, growth and mineral substrate.....	26
3.1.2 Polyurea microcapsules .....	26
3.2 Procedures .....	28
3.2.1 Bacterial growth and spore sporulation .....	28
3.2.2 Synthesis and microencapsulation .....	30
3.2.3 Material preparation to investigate encapsulation .....	32
3.2.4 Preparation of cement paste specimens .....	33
3.3 Characterization Tools .....	35
3.3.1 Chemical .....	35
3.3.2 Thermal tests.....	36
3.3.3 Microstructural.....	36
4. RESULTS AND DISCUSSION.....	36
4.1 Bacteria Viability and Growth .....	37
4.2 Synthesis and Microencapsulation of Bacteria and Nutrition.....	38

4.2.1	Chemical characterization.....	38
4.2.2	Thermal analysis .....	41
4.2.3	Microstructural analysis.....	43
4.3	Proof of Successful Bacterial Germination.....	45
4.4	Proof of Successful Calcium Carbonate Precipitation .....	47
4.5	Proof of Crack Healing .....	51
4.5.1	Crack healing tracking .....	51
4.5.2	Microstructural analysis of precipitated calcium carbonate .....	52
5.	CONCLUSIONS AND RECOMMENDATIONS.....	56
	References.....	58

## List of Tables

Table 1: Mechanisms of autogenous self-healing .....	6
Table 2: Summary of healing agent and material for capsule used in developing self-healing concrete (After improvement from [83]).....	12
Table 3: Summary of the common self-healing approaches for cementitious material.....	23
Table 4: Chemicals for synthesizing polyurea capsules .....	28
Table 5: Viability of <i>B. pseudofirmus</i> during culture and sporulation .....	37
Table 6: Thermal stability characterization of synthesized microcapsules and calcium lactate .....	41
Table 7: OD <sub>600</sub> measurement results after 0, 24 and 48 h of incubation.....	46
Table 8: TGA weight loss for synthesized microcapsules and calcium lactate .....	47
Table 9: Summarized Compressive and Flexural Strength Results for Samples.....	57

## List of Figures

Figure 1: Performance of self-healing concrete compared to traditional concrete [22].....	2
Figure 2: Flowchart of the key research activities .....	5
Figure 3: Potential autogenous self-healing mechanisms [8]. .....	6
Figure 4: Crack closing rate for different concrete mix design at W/B ratio of 0.4 [35]. (Mean and standard deviation represented by dots and error bars, respectively) (50 BFS: 50% replacement of BFS by cement).....	8
Figure 5: Schematic view of autonomous self-healing using capsule .....	10
Figure 6: Self-healing based on vascular system: (A) single channel; (B) multiple channels. Healing agent discharged from the tank through vascular to the damaged zone due to capillary and gravitational forces.....	14
Figure 7: Viability of bacterial spores ( <i>B. cohnii</i> ) in cement paste with curing time [24].....	21
Figure 8: Tests and techniques used for evaluation of self-healing efficiency as found the compiled literature [18]. .....	22
Figure 9: Preparation of <i>Bacillus pseudofirmus</i> spores: (a) incubation of media; (b) cloudy media which indicates bacterial growth after 72 hours; (c) centrifugation of culture media to obtain spore pellet and (d) centrifugation and washing spore pellets. ....	29
Figure 10: Bacteria spores: (a) dried using freeze-dryer machine; (b) crushed using ball mill. ....	30
Figure 11: Filtration and oven drying of microcapsules (Batch-1).....	31
Figure 12: schematic illustration of synthesizing and encapsulation of bacteria in polyurea capsule. .	32
Figure 13: Material preparation for investigation of encapsulation and calcium carbonate precipitation: (a) synthesized microcapsules; (b) ball bearings for crushing microcapsules; (c) powder of crushed microcapsules; (d) pouring crushed microcapsules in flasks of water and LB. ....	33
Figure 14: Casting of cement paste specimens with the artificial notch. ....	34
Figure 15: Crack creation using three point bending method .....	35
Figure 16: Single colonies obtained from serial dilution of bacteria in LB medium: (a) Typical dilution results showing lawn (uncountable) growth diluted to manageable counts (Photo courtesy of Kansas State University department of physics); (b) colonies observed on the plate obtained from our 7 <sup>th</sup> dilution. ....	37
Figure 17: Synthesized polyurea microcapsules using bacteria, calcium lactate and LB as core material .....	38
Figure 18: FT-IR spectra of the encapsulated bacteria, calcium lactate and LB in polyurea microcapsules.....	39
Figure 19: Raman spectra of Batch-1 and pure polyurea capsule with Raman shifts (a) 0 to 1000 $\text{cm}^{-1}$ ; and (b) 670 $\text{cm}^{-1}$ to 730 $\text{cm}^{-1}$ . ....	40
Figure 20: XRD patterns of Batch-1 and polyurea capsule .....	41
Figure 21: Thermal analysis of: (a) Batch-1, microencapsulated bacteria and calcium lactate in polyurea capsule; (b) polyurea microcapsules. ....	42
Figure 22: Thermograms of Batch-1 and pure polyurea capsules using second heating rate .....	43
Figure 23: Size distribution of synthesized microencapsulated bacteria and calcium lactate in polyurea capsules (frequency is expressed as a percentage of particles falling within each size range). ....	43
Figure 24: Synthesized microcapsules have irregular shapes with many protrusions and holes due to release of $\text{CO}_2$ :(a) Batch-1;(b) pure polyurea capsule.....	44
Figure 25: EDX analysis which confirms the presence of calcium lactate: (a) Batch-1; (b) pure polyurea. ....	45
Figure 26: Preparation of samples for optical density measurement. ....	46

Figure 27: Images from fluorescence microscope: (a) Bacillus Pseudofirmus DSMZ 8715 spores; (b) bacterial spores germinated in M1 (LB) after 24 h; (c); (d) bacteria spores germinated in M2 (water) after 24 h .....	47
Figure 28: TGA graphs of pure polyurea capsule, crushed capsules incubated in water, LB and calcium carbonate .....	48
Figure 29: FT-IR spectra of the dried particles after 8 day incubation in water and LB .....	49
Figure 30: XRD spectra of dried particles obtained from incubation of crushed capsules in LB and water.....	50
Figure 31: EDX analysis of dried solids by point analysis confirms precipitation of calcium carbonate .....	50
Figure 32: Crack creation using three-point bending/flexural test (after 7 day curing).....	51
Figure 33: Crack healing of cement paste specimen as a result of the microbial precipitation of the calcium carbonate .....	51
Figure 34: Dino Lite microscopy image of the crack filled with precipitation of calcium carbonate at magnification factors of: (a) 50X; (b) 230X. ....	52
Figure 35: precipitated white particles which was analyzed by FE-SEM and EDX at magnification of: (a) 30X; (b) 500X.....	53
Figure 36: EDX analysis of precipitated crystals confirm presence of Ca element in all spectra (results are in weight % - only Spectrum 1 is shown). ....	53
Figure 37: Ettringite crystals of cement paste: (a) control sample; (b) from literature [148]. ....	54
Figure 38: TGA graphs of the cement paste: (a) healed; (b) pure. ....	55

## List of Abbreviations

ASTM	American society for testing and materials.
B	Bacillus
BFS	Blast furnace slag
C <sub>4</sub> A <sub>3</sub> S	Calcium sulfoaluminate
Ca	Calcium
CaC <sub>6</sub> H <sub>10</sub> O <sub>6</sub>	Calcium lactate
CaO	Calcium oxide
Ca(OH) <sub>2</sub>	Calcium hydroxide
CaCO <sub>3</sub>	Calcium carbonate
CaSO <sub>4</sub>	Calcium sulfate
CO <sub>2</sub>	Carbon dioxide
DSC	Differential scanning calorimetry
DSMZ	German collection of microorganisms and cell cultures
ECC	Engineered cementitious composites
EDX	Energy-dispersive spectroscopy
FA	Fly ash
FE-SEM	Field emission scanning electron microscope
FT-IR	Fourier transform infrared spectroscopy
MICP	Microbial induced calcium carbonate precipitation
MCB	Mineralization controlled biologically
MIB	Mineralization induced biologically
Na <sub>2</sub> SiO <sub>3</sub>	Sodium silicate
LWA	Light weight aggregate
OD <sub>600</sub>	Optical density at 600
OPC	Ordinary portland cement
PU	Polyurea
SAP	Super absorbant polymer
SHC	Self-healing concrete
TGA	Thermogravimetric analysis
XRD	X-ray diffraction

## **1. INTRODUCTION**

### **1.1 Background**

Concrete is the second most consumable material in the world next to water. Concrete dominance in the construction industry is attributed to its high compressive strength, excellent durability, abundance and affordability [1]. However, cracking in concrete can occur at any stage of its service life for a wide range of reasons including shrinkage, chemical attacks, inadequate design or faulty construction. Billions of dollar are spent annually on the maintenance of concrete infrastructures [2]. Micro cracks do not necessarily affect concrete strength, but they can impair its durability and long-term permeability [3, 4]. The presence of cracks allows easy access for oxygen, water and detrimental chemicals responsible for concrete degradation, rebar corrosion and loss of structural integrity.

Self-healing of concrete (SHC) is an effective solution to minimize the cost of rehabilitation and subsequently increase the service life of the structure (Figure 1). As the name implies, self-healing provides unassisted healing of cracks in concrete, i.e. without human intervention (repair work). Pioneered by Dry in 1990, several approaches were proposed for self-healing in concrete. Over the last 25 years, self-healing of concrete has been extensively investigated. Self-healing techniques are classified as either autogenous or autonomous [5-7]. The former referred to as the ability of the cementitious material to recover (heal) naturally after the appearance of cracks via continuous hydration, calcium carbonate formation, and clogging of pathway by fine particles accumulation [4, 8-10]. However, natural healing is limited to crack widths of 0.1 mm to 0.3 mm [11-14]. In autonomous self-healing, a specifically designed healing agent is incorporated into the concrete mix to enhance the capacity of self-healing. Different techniques have been adopted for this purpose, such as encapsulation of adhesives and chemicals [15-18], expansive materials and mineral admixtures [19-21].

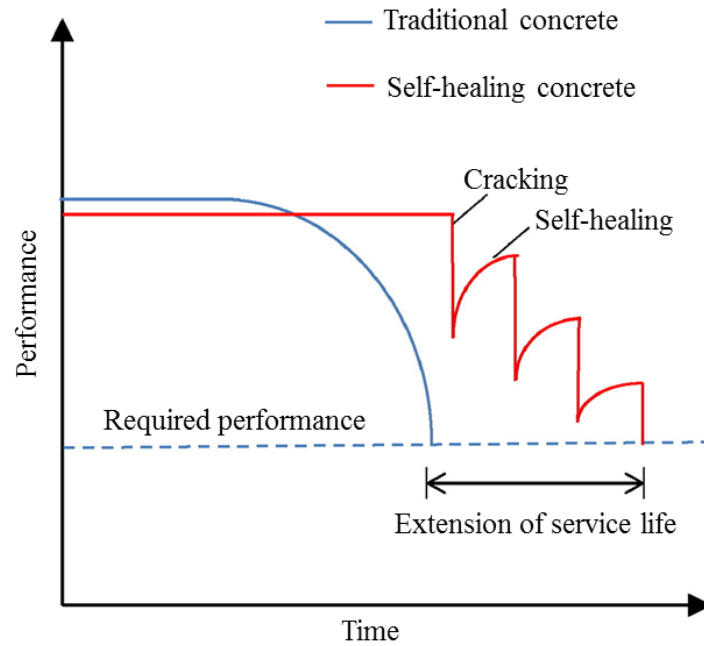


Figure 1: Performance of self-healing concrete compared to traditional concrete [22].

While most of the healing agents are chemical-based, bio-treatment approaches have shown high potential to self-heal cementitious media. In bio-healing, bacteria produces a compatible material (limestone) through a bio-chemical process referred to as microbologically-induced calcium carbonate precipitation (MICP) [23]. Ureolytic bacteria was used for this purpose based on the enzymatic hydrolysis of urea. The main disadvantage of this type of bacteria is that two ammonium ions are produced for each carbonate ion, which is harmful for human health and environment and could exacerbate corrosion of rebar. Therefore, non-ureolytic bacteria is preferred for this purpose [24, 25]. In any event, survival of bacteria in dry and alkaline condition prevalent in concrete is instrumental for successful self-healing. The viability and survivability of live cells and spores in concrete were studied. Direct inclusion of bacteria cells into concrete jeopardizes their viability due to the continuous hydration of the cementitious material and the vulnerability to crushing under the compressive stresses [26]. Therefore, addition of unprotected cells and spores into the concrete mix is not feasible. As such, long-term protection of the bacterial cells and spores is inevitable for chemical and mechanical shielding. Inclusion of bacteria is performed either via encapsulation or

impregnation. Microcapsules have shown a potential to carry bacteria, nutrition and precursors [27, 28].

### **1.2 Problem Statement**

Chemical-based agents used for self-healing of concrete suffer from a number of shortcomings. For instance, toxicity and expiry date of chemical agents and most of the chemical-based self-healing agents are two component system which can reduce the efficiency of self-healing. Therefore, there is a pressing need to utilize efficient and environmental-friendly materials and techniques for sealing cracks in concrete. Self-healing of concrete can be alternatively achieved using an appropriate type of bacteria that are known to precipitate calcium carbonate (limestone) for crack sealing. The use of bacteria as a healing agent is harmless as it is not derived from crude oil or chemical compounds. However, survival of the bacteria requires encapsulating bacterial nutrition (e.g. calcium precursor) together with an aid for spores germination (e.g. yeast extract) to ensure its growth. This is a challenging task in terms of the selection of an adequate shielding material as well as the incorporation of the nutrition and the germination aid. The capsule should have adequate physical and mechanical properties to sustain mixing with the fresh cementitious matrix and to provide adequate bonding at a later stage. For releasing the healing agent, the material of the capsule should also exhibit equal balance between flexibility and brittleness.

### **1.3 Objectives**

This research explores developing a new environmentally friendly polymeric material as a bacteria carrier and assess the potential of self-healing effect of bacteria in cement paste. Polyurea is considered for this purpose. The objectives of this research are:

1. Synthesis and encapsulation (shielding) of bacteria and nutrition in polyurea microcapsules.
2. Proof of self-healing in cement paste using the encapsulated bacteria in polyurea.

#### **1.4 Organization**

This report comprises five chapters namely; Introduction, Literature Review, Experimental Program, Results and Discussions, and Conclusions and Recommendations. Chapter 1 includes a background on self-healing concrete, the problem statement, and the research objectives. Chapter 2 presents a literature review on the concept, materials and methods of self-healing in concrete with more emphasis on bio-based techniques. Chapter 3 provides details of material selection, equipment, sample preparation, and experimental procedure. Characterization of microcapsules and the proof of concept are discussed in Chapter 4. Chapter 5 summarizes the major findings and conclusions of the research and provides some recommendations for future studies. Figure 2 demonstrates the key research activities along with materials and the characterization tools used. The activities can be divided into two phases. In the first phase, synthesis and encapsulation of bacteria and precursors in polyurea capsule are conducted. The produced microcapsules are characterized using destructive and non-destructive techniques to ensure proper formation and functionality. The activities in the second phase evaluate the success of the bacteria encapsulation in polyurea and the ability of the microcapsules to self-heal cement paste specimens.

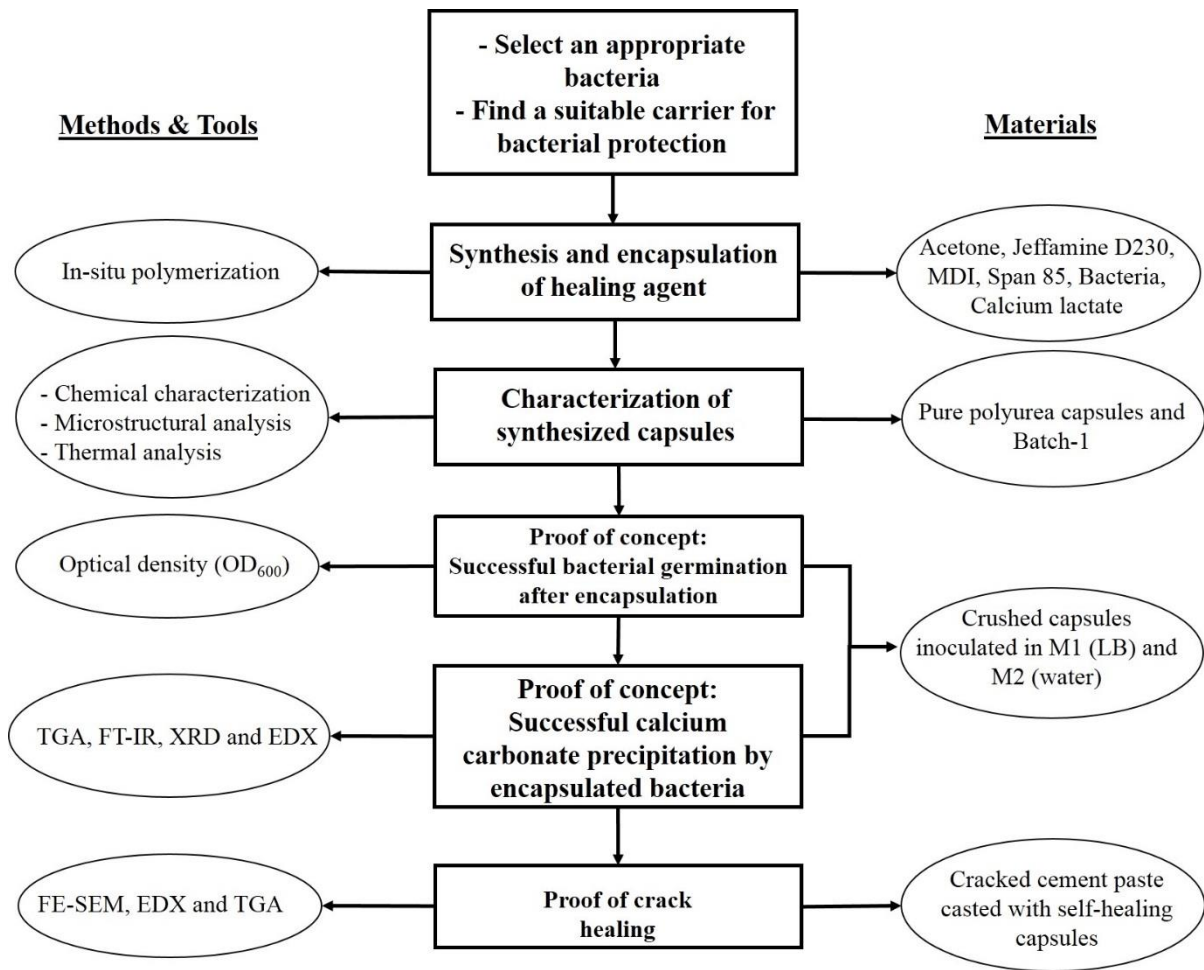


Figure 2: Flowchart of the key research activities

## 2. LITERATURE REVIEW

The International Union of Laboratories and Experts in Construction Materials, Systems and Structures (RILEM) defines self-healing as “any process by the material itself involving the recovery and hence improvement of a performance after an earlier action that had reduced the performance of the material” [6]. Concrete has been found to heal itself overtime by secondary hydration of unreacted cement particles and precipitation of calcium carbonate crystals [4, 29]. Self-healing process is categorized as autogenous and autonomous self-healing.

### 2.1 Autogenous Self-Healing

Autogenous self-healing refers to as the ability of a cementitious material to recover or heal its cracks typically upon hydration of unhydrated cement particles. Figure 3 schematically depicts potential autogenous self-healing mechanisms. Further details on the mechanisms are summarized in Table 1.

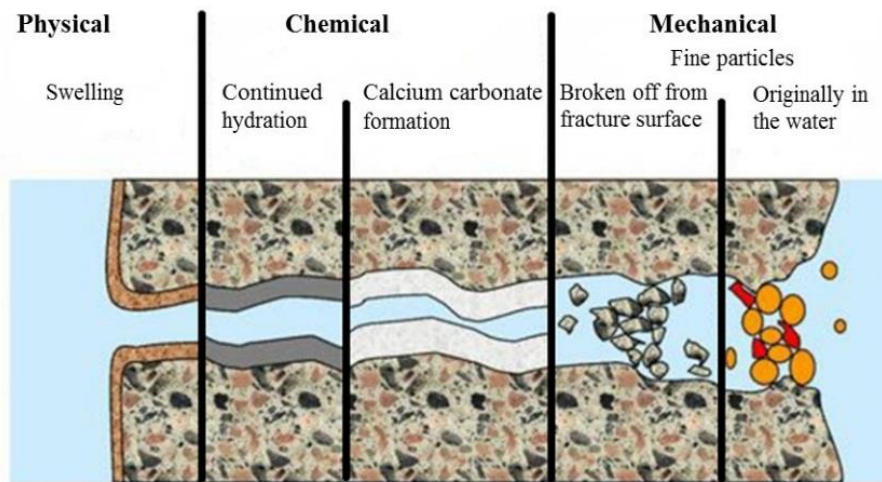


Figure 3: Potential autogenous self-healing mechanisms [8].

Table 1: Mechanisms of autogenous self-healing

Mechanism	Description/Type	Note
<b>Physical</b>	Swelling of interior material	affected to hydration of cement paste
<b>Chemical</b>	Hydration of unhydrated cement Chemical reaction between carbon and calcium ions	triggered by water triggered by water; pH and temperature affects the performance
<b>Mechanical</b>	- Migration of fine particles which can engage in particle healing - Particles which are broken off from fracture surface, partially closing the crack	affected by water

Many researchers have investigated the autogenous phenomenon in the last two decades [30-33]. The concrete autogenous healing and reinforced concrete corrosion in water penetrated separation cracks were investigated in a study by Ramm and Bischoff [32]. They reported that the water pressure, the degree of water acidity and long term (2 years) pH value could influence the corrosion of reinforcement and autogenous healing of 0.1 mm width Cracks. The observations showed no corrosion instances concerning this crack width but it began to appear in respect with 0.2 mm width cracks depending on pH value. They concluded that the increase in corrosion was a function of crack width, the pH value and acid water penetration. Also they noticed that a 0.4 mm width crack in the sample and the pH 5.2 produced the highest corrosion. Yang et al. [33] investigated the autogenous self-healing for engineering cementitious composites (ECC) made of fiber during wetting-drying cycles. Results showed adequate autogenous healing of ECC in different applications under common environmental conditions.

The autogenic healing is a type of autogenous healing in case the recovery process utilizes materials components that could be used in concrete while not specifically designed for self-healing. Autogenous self-healing is evidently effective in repair cracks smaller than 300  $\mu\text{m}$  wide [34]. Accordingly, an engineering technique must be used to mitigate the crack width and enhance autogenous healing. Alternatively some agents can be introduced to the crack to enhance the autogenous healing. An effective methodology for this purpose was proposed by Van Tittelboom & De Belie [7], namely the modified autogenous self-healing. In this review it was found that supplying water to the material mixture can be made possible through addition of super absorbent polymers (SAP) in cement mixture. Water or moisture ingress into concrete crack causes further swelling of SAP and subsequently results in blocking the cracks.

Another autogenic healing technique includes fly ash (FA) or blast furnace slag (BFS) as full or partial cement replacement. These materials can promote the crystal deposition inside the cracks during the autogenous self-healing process. Van Tittelboom et al. [35] has shown that

partial substitution of FA and BFS with cement enhances autogenous self-healing. Also, Termkhajornkit et al. [36] conducted a similar research and they concluded that FA improves the autogenous self-healing capability of concrete. According to the findings by Sahmaran et al. [37], specimens containing FA have more reactive materials and consequently higher autogenous self-healing performance was expected. But the samples with BFS showed more self-healing product compared to the sample with FA. The presence of calcium hydroxide is crucial for further reaction of FA or BFS during self-healing process [38]. As shown in Figure 4, the samples with high content of FA and BFS did not improve the autogenous self-healing capacity due to the lack of calcium hydroxide for further reaction [35].

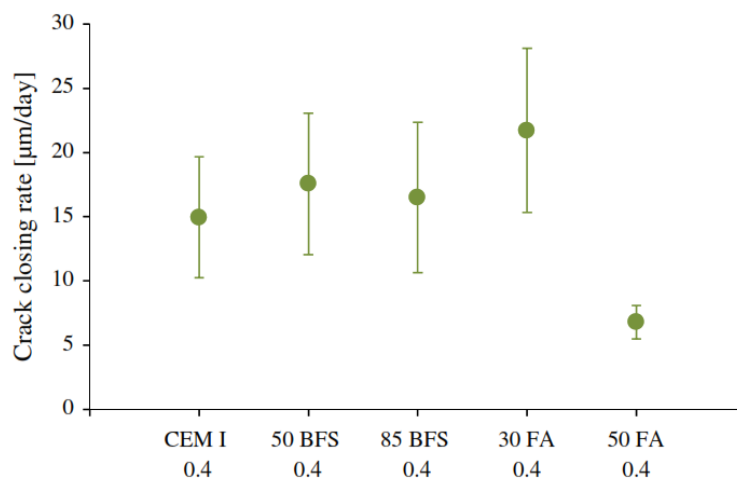


Figure 4: Crack closing rate for different concrete mix design at W/B ratio of 0.4 [35]. (Mean and standard deviation represented by dots and error bars, respectively) (50 BFS: 50% replacement of BFS by cement)

## 2.2 Autonomous Self-Healing

Restoring damaged concrete using autonomous self-healing can be achieved using a number of agents and systems. Protection and delivery of healing agents in concrete can be achieved by the means of capsules or vascular systems. The following sections concisely describes the materials used as healing agent and protection in previous studies:

### 2.2.1 Using capsules

Microencapsulation technique was first introduced in 1950s and was applied in various construction materials and industries including food, pharmaceutical, textile and chemical

products [39]. Three techniques can be used to prepare microcapsule [39]: Polymerization, coacervation technique, and mechanical methods. The microcapsule diameter and thickness are the key design considerations. The self-healing microcapsule approach can resolve problems related to the interior and micro-scale cracking. The self-healing material (agent) is discharged in the cracked area through capillary and gravitational forces, subsequent to capsule (carrier/shield) rupturing due to crack propagation. The self-healing microcapsule process (healing agent polymerisation) are favourable because of the low shrinkage rate throughout polymerisation, long life expectancy and minimal viscosity [40].

A number of studies were undertaken to apply the autonomous self-healing phenomena in concrete. The most widely used methods for this purpose are the bacterial spore encapsulation [24, 27, 40, 41] and chemical encapsulation [15-18, 42-48]. In a pioneering pilot study, White et al.[40] proposed a microencapsulated healing agent in capsules that was released once the crack rupture the capsule. The polymerization of the healing agent occurs once it is in contact with the embedded catalyst and subsequently the crack is closed. Their experimental results showed that 75% toughness recovery was achieved.

Shape of capsules could be cylindrical or spherical. Figure 5 shows the schematic view of autonomous self-healing using capsule. Numerous studies [49-57] investigated the impact of capsule size and content on the mechanical properties of cementitious materials including the deflection limit, flexural strength and stiffness. The mechanical properties of concrete such as compressive strength recovery and ductility were examined after self-healing by Pelletier et al. [18]. They used microcapsule with shell material of polyurethane and healing agent was sodium silicate solution. The microcapsules with varying sizes from 40-800 microns mixed in the concrete by 2% water volume. The outcomes demonstrated that the concrete specimens with microcapsules could recover 26% and control sample could recover 10% of their initial value after 1 week. In addition, the samples containing capsule demonstrated that the corrosion

was dramatically decreased while the compressive strength was not affected by the presence of capsules.

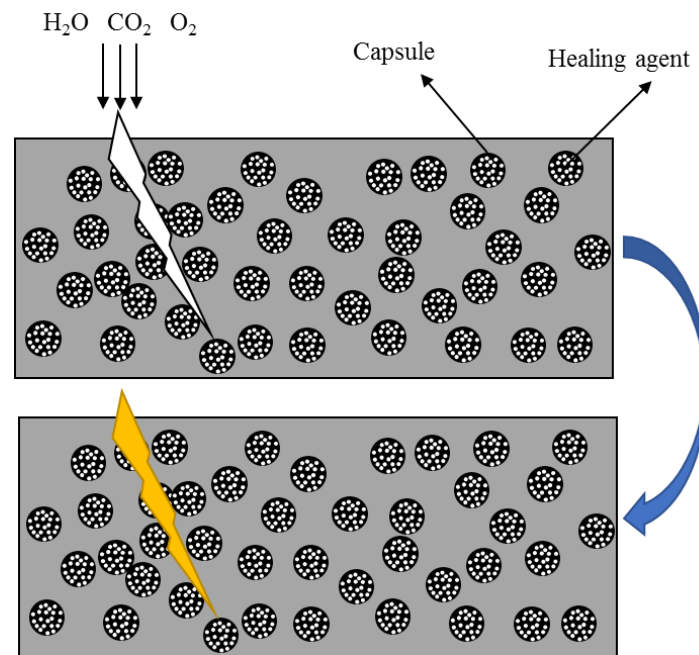


Figure 5: Schematic view of autonomous self-healing using capsule

Jonkers and Wiktor [58] inserted biochemical agents into permeable expanded clay aggregates. The expanded clay aggregates were substituted partially by normal aggregates in concrete mix. They have shown that a 100-day water curing has healed crack widths up to 0.46mm in cement sample containing bacteria, as opposed to healing cracks up to merely 0.18 mm in a control sample. Yang et al.[59] proposed another group of self-healing microcapsules comprised of oil as core material and silica gel as the shell material. They synthesised microcapsules with an average diameter of 4.15  $\mu m$ . Methylmethacrylate monomer and triethylborane were adopted as healing agents and oil as core material acts as catalyst. The self-healing efficiency of mortars specimens which contained microcapsules and microfibers were assessed utilizing permeability and fatigue test under uniaxial compressive cyclic loading. Results demonstrated that gas permeability of cement mortar samples with microcapsules were improved, which indicates self-healing by microcapsules. However, the fatigue test results showed that the crack

resistance were improved by the addition of small content (dosage) of microcapsules into carbon microfiber reinforced mortar.

Numerous studies [60-64] have contemplated the impact of cylindrical or capsules' content and size on mechanical properties of concrete such as the deflection capacity, flexural strength and concrete stiffness. Van Tittelboom et al. [65] used two types of tubular capsules containing MEYCO MP 355 1K resin (BASF The Chemical Company) as healing agents and examined their effectiveness. Their findings showed that both types of capsules had identical performance. Also, the damage recovery demonstrated the suitability of the healing agent. Van Tittelboom et al. [66] utilized a similar system to convey microorganisms to concrete utilizing glass tubular capsules, and protected the bacteria from the harsh environment of concrete by encapsulating them in silica gel and polyurethane. Thermogravimetric analysis (TGA) showed that precipitation of calcium carbonate from the bacteria immobilized by silica gel and polyurethane were 25% and 11% by mass, respectively. Experimental results and analysis have shown that crack in mortar specimens with immobilized bacteria in polyurethane had higher strength recovery compared to those healed by silica gel immobilized bacteria. Table 2 summarizes common materials (agents) and capsules used for self-healing of concrete.

Table 2: Summary of healing agent and material for capsule used in developing self-healing concrete (After improvement from [83])

Approach	Healing agent	No. components		Viscosity (mPas)	Capsule material	Capsule dimension ( $\mu\text{m}$ )			Source
		Single	>1			Diameter	Thickness	Length	
<b>Encapsulation of chemical agent</b>	Cyanoacrylate (CA)	1	-	<10	Glass	800 1500 300	X X X	75 75 100	[17]
	CA	-	2	<10	Glass	2000-3000	100	20-80	[67]
	Epoxy	-	2	150 80 360	Glass	2000-3000	100	20-80	
	Epoxy	1	-	250-500	Glass	5000 6000 7000	X	250 250 X	[50]
	Epoxy	-	2	X	Perspex UFF	X 20-70	X	X NA	[68]
	Acrylic resin	-	-	X	Gelatin	125-297	X	NA	
	Epoxy	-	2	200	UF	120	4	NA	[69]
	Sodium silicate solution	1	-	X	PU	40-800	X	NA	[18]
	MMA with TEB at catalyst	-	2	1	Silica gel	4.15	X	NA	[59]
	Epoxy	1	-	X	Gelatin	50	X	NA	[45]
	Tung oil	1	-	X	Gelatin	50	X	NA	
	Calcium hydroxide	1	-	X	-	50	X	Na	
	Polyurethane	-	2	600	Glass	2200	100	20-80	[16]
	PU	-	2		Ceramics	3350		15-50	[70]
	Sodium silicate	1	-	X	Glass	3350	350	50	[71]

	Epoxy resin E-51	-	2	X	Urea-formaldehyde	132, 180 and 230	NA	NA	[72]
	Sodium silicate solution	1	-	X	Gelatin-acacia gum	300 - 700	5-20	NA	[73]
	silanol-terminated polydimethylsiloxane (STP)	1	-	X	Urea-formaldehyde	220	X	NA	[74]
	dibutyltin dilaurate (DD)	1	-	X	Polyurethane	75			
	Epoxy resin E-51	1	-	X	Melamine Urea-Formaldehyde	200	1.1 – 2.4	NA	[75]
	Sodium silicate				Polyurethane/urea-formaldehyde				
<b>Encapsulation of bacteria</b>	Bacteria and calcium lactate	-	2	NA	Expanded clay	1000-4000	NA	NA	[76]
	Bacteria	-	2	NA	PU in glass	2200	100	20-80	
	Bacteria	-	2	NA	Silica gel in glass	3350			[27]
	Bacteria	1	-	NA	Melamine	5	X	NA	
	Bacteria	1	-	NA	Hydrogel	NA	NA	NA	[77]
			-	2	NA		NA	NA	
	Bacteria	1	-	NA	Diatomaceous earth (DE)	X	NA	NA	[78]
	Bacteria sphaericus (Immobilization)	1	-	NA	Biochar	X	NA	5-120	[79]
	Bacteria Sposarcina ureae and Sposarcina pasteurii	1	-	NA	zeolite clinoptilolite	NA	NA	620	[80]
	Bacteria (Immobilization)	1	-	NA	Magnetic iron oxide nanoparticles	NA	NA	X	[81]

### 2.2.2 Using vascular system

Autonomous self-healing by vascular system is defined as filling healing agents in empty fibres or tubes that are able to connect the internal and external of the structure using vascular system. In this system, the healing agent can be transported to the damage zone by single or multi-channel system as shown in Figure 6. Accordingly, upon occurrence of crack, the healing agent is discharged and goes to the damaged zone and creates bonds with the primary structural material

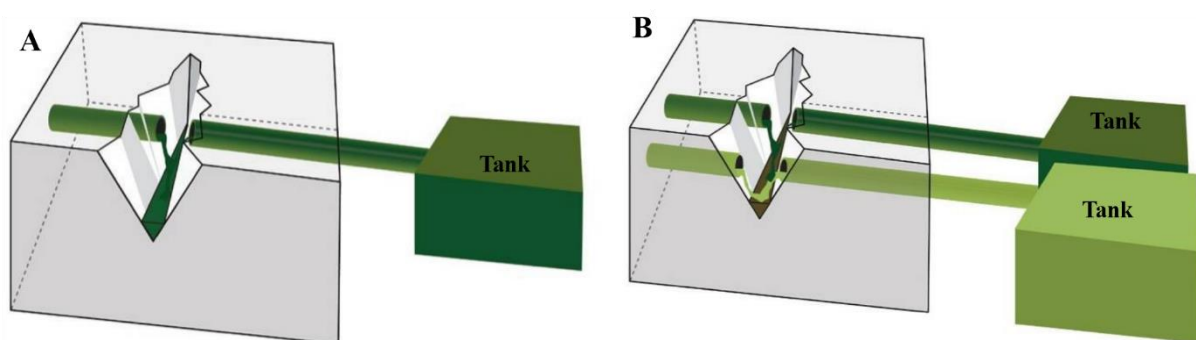


Figure 6: Self-healing based on vascular system: (A) single channel; (B) multiple channels. Healing agent discharged from the tank through vascular to the damaged zone due to capillary and gravitational forces

Different researchers [82-85] have considered utilizing various healing agents for quite a long time. Sangadji and Schlangen [83] employed an alternate procedure, which endeavoured to mimic the bone healing procedure. Their exploratory method included a porous system for simulating the 'spongy bone' by placing porous concrete within the concrete. They inserted the healing agents manually at the damaged area of cylindrical and beam samples after crack creation. The self-healing results evidently recovered the strength of concrete.

Sun et al. [46] investigated the effectiveness of self-healing of hollow glass fibers filled with healing agent on the small cracks of a concrete bridge. The impact of glass reservoirs in terms of length of and diameter on the self-healing was examined by Joseph et al. [17]. Also, they investigated the effect of loading rate and reinforcement level on the coverage of self-healing. They concluded that self-healing occurred during the first and second load cycles. Dry [15]

compared the success/efficiency of self-healing using manual resin injection in the cracks versus that of the inclusion of the adhesive material (healing agent) in the concrete mix. The results suggest that the manual resin injection method has a number of advantages, such as controlling the area of injection. Kuang et al.[86] explored the recycle of static loads on concrete beams using shape memory alloy (SMA) wire that acted as reinforcement and fragile fibres with adhesive content. Findings indicated that this method enhanced self-recovery potential of concrete beams.

### **2.3 Biotechnology for Self-Healing**

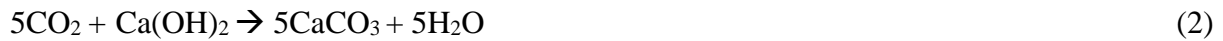
Biotechnology plays a vital role in construction as it does in other industries, such as materials production or petroleum engineering. Biotechnology developed modern materials such as bio mortar or concrete or bacterial concrete to improve longevity. Self-healing of concrete using bacteria refers to using bio-compound agents to expand the life expectancy or durability via healing the cracks in the concrete. Bacteria is perceived as an external repair material whereby the microorganisms are added to the concrete mix. Self-healing efficiency is typically evaluated through the improvement in strength and permeability. Materials made of chemical synthesis like epoxies are utilized for repairing concrete cracks, yet such repair entails various drawbacks. They differ thermal expansion coefficients relevant to the concrete and pose some level of risk to the environment and human wellbeing. As an alternative, self-healing of concrete based on precipitation of calcium carbonate is considered as an environmentally friendly approach. Self-healing of concrete by bacteria is viewed as a favourable answer for concrete cracks to substantially decrease the high repair expenses.

MICP involves insertion of bacteria and precursors in concrete to produce minerals (calcium carbonate) to heal the cracks. It occurs mainly due to metabolic conversion of the organic source, such as calcium lactate to produce calcium carbonate. Unlike ureolytic metabolic conversion, this process does not produce high amount of ammonia, which is hazardous and

equally exacerbates corrosion of steels rebars [87]. Equation (1) shows bacterial metabolic conversion of the calcium lactate [87] :



On the other hand, calcium carbonate precipitation increases when the produced carbon dioxide ( $\text{CO}_2$ ) reacts with the cement hydration products, portlandite ( $\text{Ca}(\text{OH})_2$ ) as follows:



### **2.3.1 Bio-mineralization of bacteria**

MICP as a bio-mineralisation mechanism occurs either through mineralization controlled biologically (MCB) or mineralization induced biologically (MIB) [88]. Calcium carbonate production can result from a natural or synthetic procedure through microbial metabolism. MICP is a biochemical mechanism, having four major factors to accomplish the procedure by the microorganisms; (a) calcium concentration to develop calcium carbonate, (b) concentration of the dissolved carbon for precipitation of calcite, (c) the pH level and the accessibility to nucleation points (site), and (d) the microorganism's capacity for nucleation. The precipitation of  $\text{CaCO}_3$  relies upon the solubility constant ( $K_s$ ) and the product of ion activity ( $kiap$ ). In the event that  $kiap > K_s$  the system is faced with oversaturation and there is potential for the precipitation [89]. Natural precipitation of calcium carbonate occurs as a result of a number of processes:

1. Chemical precipitation as a result of evaporation from saturated solution under the effect of temperature increase and/or decrease of the pressure.
2. External and internal skeleton Production by the eukaryotes.
3. Pressure derivation of  $\text{CO}_2$  under the autotrophic processes' effect.
4. Fungi involvement.
5. Bacterial involvement.

### **2.3.2 Biology basis**

Over the last two decades, the development of biological mortar exploited the knowledge bio-concepts aiming at sealing small cracks in concrete and cavities on stone surfaces. Biological mortar is composed of three core components bacteria, nutrients and limestone powder [90]. Obtaining adequate mortar, the three core components of biological mortar dosage were optimised, counteracting surface tension in the presence of micro cracks and towards rupturing. In order to assess different parameters of biological mortar during the in vitro experiments, the finest percentage was obtained using 25% of bacterial paste (containing  $10^9$  cells  $\text{mL}^{-1}$ ), 25% of nutritional medium, and 50% of limestone powder with 40-60  $\mu\text{m}$  stone particles. The mortar was applied to the Amiens Cathedral sculptures and the church portal of Argenton-Château, France, and verified in small scale. After two years of treatment, the findings indicated a satisfying appearance in the mended areas [56].

### **2.3.3 Self-healing using bacteria**

Biochemical agents are used to make concrete, along with incorporation of microorganisms and agents into concrete mixture to extend the longevity or the durability of concrete structures through sealing the cracks. The consequences of direct supply of these materials to the mix are yet unknown with confidence. This includes the mechanical properties of the concrete, durability.

The remediation of concrete using *B. pasteurii*, nutrients and sand as the filling material was investigated by Ramachandran et al. in 2001 [91]. The compressive strength and stiffness values of the biologically-treated samples were significantly higher than those with no microbiological preparation. Furthermore, a range of filling materials was used to seal cracks and to examine their impacts on the efficiency of fixing cracks (Day et al.) [92]. Concrete beams treated using bacterial and polyurethane had higher stiffness than those involving a mixture sand, lime, FA, and silica as filling materials. The ability of *B. sphaericus* with ceramic as a filling material to seal concrete cracks was studied by De Belie and De Muynck [93]. *B.*

*sphaericus* was protected from the high pH in concrete through immobilization of the bacterium in a silica solution provided with additional salt levels. Samples rectified by bacteria with ceramic were the same as those remedied by epoxy injection, both of which decreased water permeability.

Application of microbiological processes significantly promoted the compressive strength [27, 91, 94, 95]. Besides, microbiological treatment resulted in improved surface of concrete because of decreased water absorption rate [54, 96]. The ability of bacteria, its nutrients, and precursor on surface finish as a biocompatible approach was examined to fix concrete cracks rather than traditional methods (Richardson et al.) [97, 98]. They observed *S. pasteurii* to be capable and consequently MICP to enhance the integrity of completion to concrete, in the absence of chemical based sealants. Their results also showed that *S. pasteurii* could seal micro-cracks to a depth of approximately 20 mm.

Ramakrishnan were first to investigate bacteria-based self-healing concrete to increase the compressive strength of cube mortar samples. Ramakrishnan et al. [91] casted mortar samples with dimensions 50.8×50.8×50.8 mm, containing 660g of sand, 240g of cement, and 16.4 ml of *B. pasteurii* suspended in phosphate buffer [91]. After 24 h, all samples were demoulded and remedied in a medium of urea-CaCl<sub>2</sub> for 7 and 28 day. A significant increase was observed in compressive strength, especially in the 28-day samples, confirmed by Achal et al. as well [99] The impact of incorporating *Shewanella* on the compressive strength of mortar samples was explored by Ghosh et al. [100]. Their experiment aimed at curing the samples in air rather than a medium containing nutrients. For all samples, the water-cement ratio and the concentration of bacterial cells were 0.4 and 10<sup>5</sup> cell mL<sup>-1</sup>, respectively. Following 28 day, they detected an elevated compressive strength of 25% in comparison with control samples.

Both bacteria and nutrients are embedded into the concrete matrix through microcapsules, vascular network, and/or combined microcapsules and vascular methods in order to yield self-healing concrete. Jonker and Schlangen (2007) first applied of self-healing concrete as an autonomous healing method [101]. They realized the bacterial strains *Bacillus pseudofirmus* DSM 8715 and *Bacillus cohnii* DSM 6307 to be the most favourable likely capable of prolonged survival in the concrete. Initially, the bacteria as spores were directly incorporated into the concrete mix, because bacterial spores are able to resist extreme chemical and mechanical stresses; then calcium lactate was inserted as a nutrient for bacteria. According to the results of ESEM scan, immense amounts of  $\text{CaCO}_3$  precipitates were present in the samples of the 7<sup>th</sup> day.

Spores are the encapsulated form of bacteria and their nutrients to be shielded against forces while being mixed with by clay particles or by suitable sand for mending cracks. Crack healing improvement was demonstrated previously using this approach [76, 102, 103]. A report by Wiktor and Jonkers [58] indicate that this technique can heal a maximum crack width of 0.46 mm, with a limited viability of the spores. Jonkers [76] observed the viability of encapsulated spores for a minimum of six months. Seifan et al. [81] immobilized bacteria on iron oxide nanoparticles and the results have proven that the concrete supplemented by magnetic immobilized cells had higher resistance to water penetration comparing to normal concrete (the initial and secondary water absorption rates in bio-concrete were 26% and 22% lower than the control specimens). Wang et al. [27] also researched the feasibility of protecting bacteria through concrete mixing and casting through the ability of silica gel and/or polyurethane. Their findings have proven that  $\text{CaCO}_3$  precipitation by bacteria immobilized in silica gel was higher than bacteria immobilized in polyurethane. Accordingly, the deficiencies of immobilisation by bacterial encapsulation in silica gel, hydrogel, expanded clay, metakaolin, zeolite and granular activated carbon were highlighted by Ersan et al. [104]. Zhang et al. [105] introduced

expanded perlite as a novel carrier for bacteria and compared his results with expanded clay. The expanded perlite has proven to be able to carry higher concentration of bacteria comparing to expanded clay [105]. Consequently, a better healing capacity was shown by expanded perlite (maximum healed crack width by expanded perlite and expanded clay reported as 0.45 mm and 0.79 mm, respectively).

There are reports on the survivability of bacteria implanted in silica gel under severe conditions where the bacteria were immobilized using hydrogel [77, 106]. The hydrogel-treated bacteria were observed to be capable of filling crack widths up to 0.5 mm by CaCO<sub>3</sub> precipitation, resulting from the excess water of the swollen hydrogel. In a moistened environment such as underground or water-containing structures, the method of bacterial spores shows promising efficiency.

#### **2.3.4 Challenges**

A number of challenges has been encountered/associated with the use bacteria-based self-healing techniques in concrete [107]. The challenges are mostly associated with the ability of bacteria to germinate, survive, and grow in the extreme unfavourable conditions present in concrete [24, 108-112]. There are reports on the survivability of live bacterial cells and their spores in concrete. The spores of *Bacillus cohnii* were directly embedded into cement paste by Jonkers et al. [24] to determine the viability period of the spores in a high alkaline environment showing that bacteria spores were able to survive up to four months (Figure 7). The researchers, however, suggested that live bacterial cells had a limited viability in a similar condition to spores due to the cement hydration process and early strength stresses, crushing the micro-sized cells. The non-alkaliphile live cells of *Rhodococcus ruber* was directly added to a magnesium phosphate cement (MPC) by Soltmann et al., indicating no effect of pH on viability with the cement hydration being the main factor [109]. They further detected that *R. ruber* survived for 19 days, even at a near-neutral pH of the cement. Also, *Bacillus megatarium*

ATCC 14581 was mixed with Portland cement (PC) paste and PC paste (with varying levels of fly ash) by Achal et al. [110]. They reported that the count of surviving cells rose with increasing levels of fly ash in the paste. The cell viability of cyanobacteria *Synechococcus* PCC8806 in the cement solution was studied by Zhu et al. [363] and it was confirmed that *Synechococcus* PCC8806 was viable lacking any protection at a pH level of 11.7. Evidence of some research attempts [315,364] signifies that *Synechococcus* PCC8806 survived in a variety of unfavourable milieus including concrete, desert settings, and oligotrophic lakes. Yet, research is needed to determine its survival for extended periods.

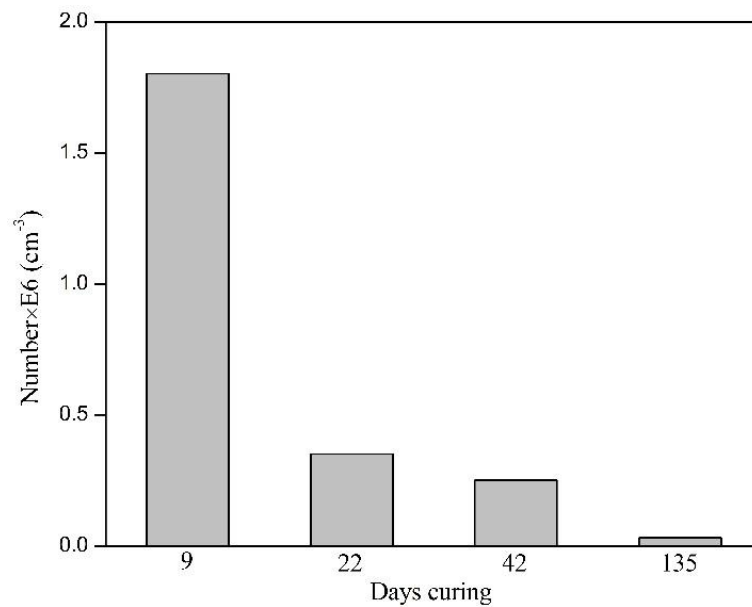


Figure 7: Viability of bacterial spores (*B. cohnii*) in cement paste with curing time [24]

#### 2.4 Summary of Self-Healing Attempts

In the last two decades a few methodologies have been developed to enhance concrete longevity through utilizing self-healing procedures. Establishing a standard methodology for assessment of the effectiveness of self-healing has been a key objectives of studies in this domain [113]. Permeability test, stress tests and scanning electron microscopy (SEM) have been employed for this purpose. These tests are performed to evaluate recovery of the

mechanical properties, fixing (healing) cracks and to examine the chemical compounds separately (Figure 8).

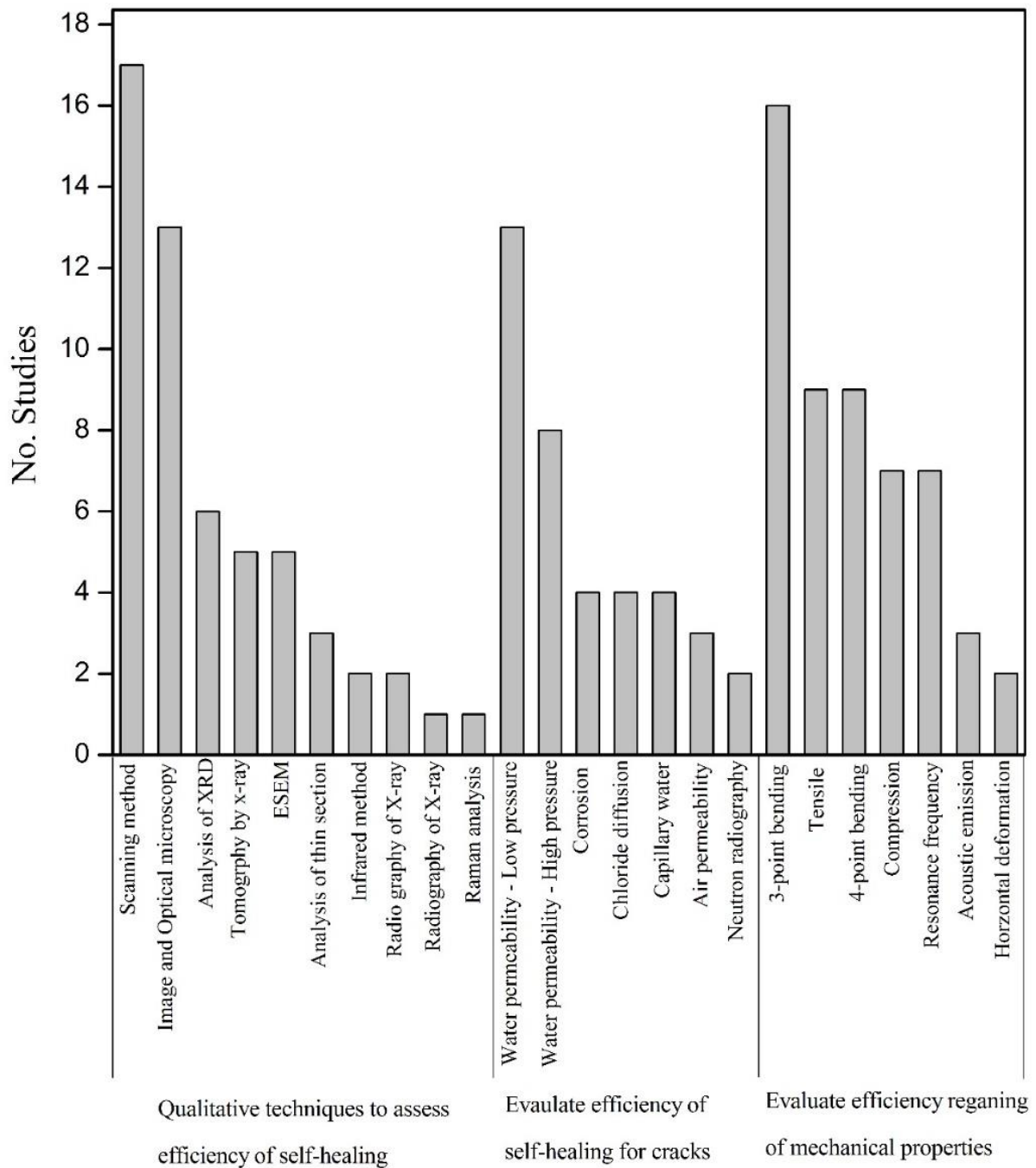


Figure 8: Tests and techniques used for evaluation of self-healing efficiency as found the compiled literature [18].

The foregoing discussion provides an overview of various approaches that allow quantitative assessment of various self-healing approaches, bacterial encapsulation and fixing the crack,

chemical encapsulation, chemical substance in glass tubing, and mineral admixture. A summary of different approaches is shown in Table 3.

Table 3: Summary of the common self-healing approaches for cementitious material

Approach	Advantages	Disadvantages
<b>Intrinsic self-healing</b>	<ul style="list-style-type: none"> <li>- Environmentally friendly</li> <li>- Lower costs</li> <li>- Broad distribution of healing agent</li> <li>- Gaining tightness and strength after healing</li> </ul>	<ul style="list-style-type: none"> <li>- Limited healing scale</li> <li>- High alkalinity and developing chloride atmosphere</li> <li>- Inadequate data for proper evaluation</li> </ul>
<b>Chemical encapsulation</b>	<ul style="list-style-type: none"> <li>- Prolonged service life</li> <li>- Simultaneously healing more than one defective point</li> <li>- Uniform distribution</li> <li>- Adequate concentration of healing agent</li> <li>- Regain mechanical strength after healing</li> </ul>	<ul style="list-style-type: none"> <li>- Unknown chemical bond of capsules and crack boundary</li> <li>- Low reliability due to insufficient evaluation data</li> <li>- More capsules cause less stiffness of cross section</li> <li>- Inadequate data on healing behaviour in various climates</li> </ul>
<b>Mineral admixtures</b>	<ul style="list-style-type: none"> <li>- High efficiency of healing</li> <li>- Consistency between cement and the healing agent</li> <li>- Suitable for underground applications</li> </ul>	<ul style="list-style-type: none"> <li>- Required treatment to prevent unwanted expansion</li> <li>- No guarantee to achieve good healing</li> <li>- Inadequate data for proper evaluation</li> <li>- Inadequate data on healing behaviour in various climates</li> <li>- Uniformity of distribution in the concrete mixture</li> </ul>
<b>Chemical in glass/fiber vascular tubing</b>	<ul style="list-style-type: none"> <li>- Discharge healing agent when necessary</li> <li>- Acceptable strength and tightness gain</li> <li>- Capability of conveying different healing agents</li> <li>- Healing mechanism is not affected by the external environmental</li> </ul>	<ul style="list-style-type: none"> <li>- Troublesome procedure of placing glass fibre</li> <li>- Higher number of glass fibres cause lower mechanical properties of concrete</li> <li>- Inadequate data for appropriate assessment</li> <li>- One time use</li> <li>- Possibility of breaking glass during mixing</li> </ul>
<b>Bacteria</b>	<ul style="list-style-type: none"> <li>- External Cracks can be remediated through filling the Cracks by Bacteria, nutrients and appropriate sand resulting in strength enhancements with a higher stiffness</li> <li>- By using similar Bacteria and procedure for crack healing lead to the development of biological binders and surface treatment to the stones</li> <li>- If used as remediation (external Self-healing) or as bio-concrete, they will promote the compressive strength and durability of concrete</li> <li>- Lessening the corrosion of strengthened concrete resulting from retrieval of the tightness</li> <li>- The bacterial precipitate corresponds to the original material</li> </ul>	<ul style="list-style-type: none"> <li>- Although the initial cost of biological concrete (remediation and/or amendment using bio-concrete and use of bacteria in external self-healing) is almost twice that of traditional Concrete [13], a decrease in the maintenance cost lowers the preliminary cost</li> <li>- The compressive strength undergoes a decrease following insertion of bacteria in capsules mixed with the concrete caused by a loads of capsules within the concrete</li> <li>- Both different nutrients and atmospheres are required for various bacteria</li> <li>- Forewarning on the cost: the Bacteria need to be shielded against the Concrete's high pH impacts</li> <li>- The bacterial concrete mix design lacks any identification standard/code</li> </ul>

## 2.5 A New Class of Material for Protection of Bacteria

Different materials have been used to carry healing agents in a capsule or via a vascular system.

The used material must have a number of qualities to sustain the mixing phase as well as for long-term service. There should be no interaction between the encapsulation material and

healing agent. The porosity of the encapsulation material should be kept very low in order to contain the healing agent. Alternatively, coating the porous capsule or vascular can be considered. However, the coating material should not react with the healing agent or the concrete. The main purpose of embedding capsule or tubes in cementitious material is to provide the quality of continuous self-healing of the concrete elements. Therefore, the encapsulation material should degrade prior to crack occurrence. Some materials lose their normal formation due to the presence of water and become flexible. Since water is one of the main constituents of concrete, the capsule or tube should endure aqueous environment.

Synthesis of microcapsules should be completed in a short time to prevent bacteria activation. Therefore, curing reaction of the selected polymer should be high. There are several materials that can be used for this purpose such as: epoxy, polyurethane, alginate and polyurea. For increasing curing reaction of epoxy and polyurethane, catalysts and accelerators with high concentration are applied, although the curing time is still high (5-10 mins). However, curing time of alginate is very fast, but its size and shell thickness are modest (high brittleness). Polyurea can be synthesized in a moist condition and even at low temperature (-60 to +200 °C) [114]. Comparatively, the curing system of polyurethane is negatively affected by humidity and the temperature must be more than 15 °C.

In this research, polyurea polymer is proposed to protect and carry bacterial spores and nutrition. Generally, polymers based on urea as a connecting chemical have attracted growing attention due to their intrinsic ability to provide multiple donor-acceptor bonds. These bonds cause novel arrangement of oxygen, nitrogen and hydrogen atoms in urea [115]. Polyurea systems are obtained based on nature or intensity chemical reaction between polyisocyanates (aromatic or aliphatic) and amino-terminated resin (aromatic or aliphatic), which creates urea groups strongly connected to the polymer chains through stable hydrogen bond having hydrogen bonds strongly interacting ( with the polymer chains [116-120]. Polyurea can tolerate

high pH and it has excellent thermal properties; moreover, it has a higher melting point compared to hybrids, polyurethanes and other polymers [121-123]. Due to bidentate of polyurea, the urea linkage is more resistance to hydrolysis [124]. Significant abrasion and chemical resistances of polyurea as well as vast service temperatures (-60 to 200 °C ) are among the outstanding properties of polyurea [114, 125]. In addition, polyurea like polyurethane systems are suitable in biomedical applications due to their excellent physical properties and their biocompatibility [126]. Polyurea has many advantages over other materials used to protect bacteria, such as fast curing, water and temperature insensitivity, high thermal stability and superb chemical resistance [69].

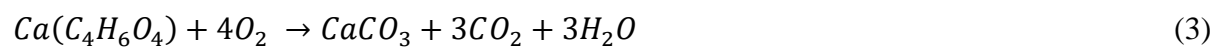
### 3. RESEARCH METHODOLOGY

In this chapter materials and methods used throughout the research will be discussed. The first section introduces the materials used to prepare the bacteria and the polyurea capsules. In the following section, methods and techniques adopted bacterial spores preparation, synthesis and encapsulation, proof of encapsulation and preparation of cement paste samples are explained in detail. Lastly, the instruments and tools used for material characterization along with their configurations and limitations are introduced.

#### 3.1 Materials

##### 3.1.1 Bacterial strain, growth and mineral substrate

Alkaliphilic *Bacillus pseudofirmus* DSM 8715 was used as a healing agent. The material, a product of the German Collection of Microorganisms and Cell Cultures (DSMZ), was stored in 50% (v/v) glycerol at  $-80\text{ }^{\circ}\text{C}$ . A standard culture technique was employed for expansion, cryopreservation and sporulation (a process to produce bacterial spores) of the bacteria [24, 25]. The bacteria was cultured in Luria-Bertani (LB) purchased from 1st BASE, which contains Tryptone 10g/L, sodium chloride 10g/L and Yeast extract 5g/L [127]. Extra pure reagent grade of calcium lactate (from Nacalai Tesque, Inc.) was chosen as a suitable organic calcium source for metabolic conversion of the bacteria to precipitate limestone [24]. The selected strain enables metabolizing calcium lactate and producing limestone and carbon dioxide by cellular respiration. The chemical reaction can be expressed as follows:



##### 3.1.2 Polyurea microcapsules

Synthesis of microcapsules should be quickly completed (within 10 to 20 minutes) to prevent activation of the bacteria and dissolving of calcium lactate and yeast extract. Therefore, curing reaction time of the selected polymer used in microcapsule should be fast. A number of materials can be considered for this purpose including epoxy, polyurethane, alginate and polyurea. Catalysts and accelerators with high concentrations are applied to increase the intensity of the curing reaction of epoxy and polyurethane. The curing time, however, is still

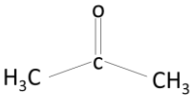
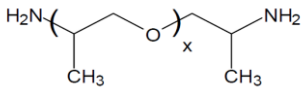
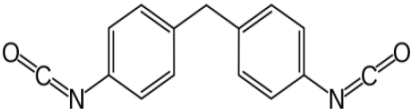
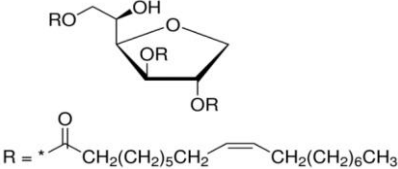
long (around 5-10 min). The curing time of alginate is very fast, but it exhibits an unsuitable brittle behavior due to the size and small shell. Hence, alginate microcapsules cannot survive and may rupture during the preparation of the cementitious mix.

The very short curing time of polyurea (approximately 8 sec) enables it to be a suitable bacteria carrier. Fabrication of the microcapsules and encapsulation can be accordingly completed quickly. Furthermore, several key properties of the polyurea are tuneable. For instance, the brittleness (or flexibility) levels of polyurea microcapsules can be synthesized just by changing the molar ratio between the hard and soft segments. The preparation of the polyurea microcapsules is not affected by the temperature and moisture variations. Polyurea can be synthesized in a moist condition and even at low temperatures (-60 to +200 °C [114]). The thermal stability and size of capsules are adjustable in the polyurea system. Several materials were used in synthesis of the polyurea capsules. The following briefly describes their key roles (Table 4).

- Acetone is used as solvent to disperse the mixture of chemical before polymerization to prepare capsules
- Diphenylmethane diisocyanate (MDI) prepolymer (NCO 15.5%) is used as isocyanate source for polyurea reaction. This type of isocyanate was selected because it provides suitable mechanical properties for polyurea matrix and also it has high reactivity during curing reaction.
- Jeffamine D230 is used as amine for polyurea reaction. The appropriate chain length of this chemical enables adjustable flexibility and brittleness of the synthesized polyurea. If the molar ratio of Jeffamine D230 is increased on formulation, the prepared polyurea capsules will be more brittle.
- Span 85 is used as surfactant. Dissolving different materials to synthesise the capsules requires using a suitable surfactant. Span 85 is used to increase the solubility of MDI in

water. Surfactants generally have two tails: one polar and another non-polar. Therefore, if an insoluble chemical mixed with water, the non-polar tail of the surfactant enhances its water solubility [128].

Table 4: Chemicals for synthesizing polyurea capsules

Name	Function	Chemical structure	Company
Acetone	Solvent		System
Jeffamine D230	Resin		Huntsman
Methylene diphenyl diisocyanate (MDI) -NCO% 15.5	Curing agent		Huntsman
Span 85	Emulsifier		Sigma Alrich

### 3.2 Procedures

#### 3.2.1 Bacterial growth and spore sporulation

Bacterial spores can survive without nutrition and they can sustain harsh environments including dryness, high temperature and extreme freezing. For this purpose, *B. pseudofirmus* was cultured in Luria Betrani (LB) broth supplemented with 4.2 g of NaHCO<sub>3</sub> and 5.3 g of Na<sub>2</sub>CO<sub>3</sub>. Growth media was adjusted to a pH value of 9.0 using 5 M NaOH and autoclaved prior to inoculation of *B. pseudofirmus* to eliminate contamination. *Bacillus pseudofirmus* spore (8715 DSMZ) was reconstituted in accordance to the vendor's instructions. The spores were suspended in 1 ml sterile LB and incubated at room temperature for 30 minutes. The suspension was then transferred to a 50 ml falcon tube containing 10 ml sterile growth media and incubated for 48 hours at 37 °C with shaking at 150 rpm. Approximately 10 µl of the original suspension was transferred to an LB agar plate (pH 9.0) and spread to obtain single colonies for use as a working stock [24, 25]. Glycerol stocks were preserved using the bacterial

cultures harvested at 48 hours post inoculation. Stocks were created by mixing 750 ml of the saturated bacteria culture with 350 ml of cryopreservation media comprised of sterile LB (as detailed above) and 50% v/v glycerol. Stocks were accordingly stored at -80 °C.

Bacteria cultures used for experiments were grown in 25 g/L of LB. The pH value of the cultures was adjusted to 9.0 using 5 M NaOH and sterilized by autoclaving for 20 min at 121 °C prior to inoculation. Flasks of growth media were then aerobically incubated at 37 °C in an incubator shaker at 150 rpm for 72 hours (Figure 9a and b). Sporulation of bacteria was achieved by incubating late log/early stationary phase bacterial cultures for an additional 24 hours (i.e. elapsed 72 hours post inoculation) and stored at 4 °C. Spores were checked for mobility using standard light microscopy and harvested by centrifugation at 7000 g for 5 min at room temperature. Finally, the cultures were washed by repeated centrifugation for 5 min at 7000 g (Figure 9 c and d). Spore pellets retrieved post centrifugation were lyophilized using a freeze-dryer for 24 hours at -40 °C (Figure 10a) [25]. The produced dehydrated spores were powdered using a ball mill for 2 min at 300 rpm as shown in Figure 10b.

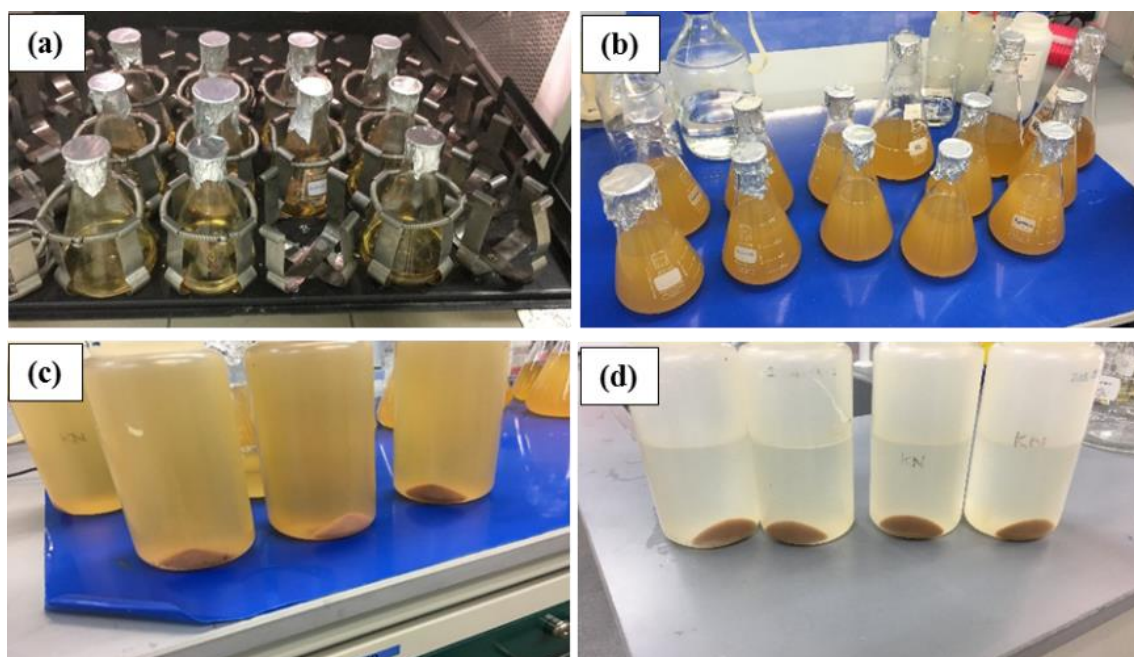


Figure 9: Preparation of *Bacillus pseudofirmus* spores: (a) incubation of media; (b) cloudy media which indicates bacterial growth after 72 hours; (c) centrifugation of culture media to obtain spore pellet and (d) centrifugation and washing spore pellets.

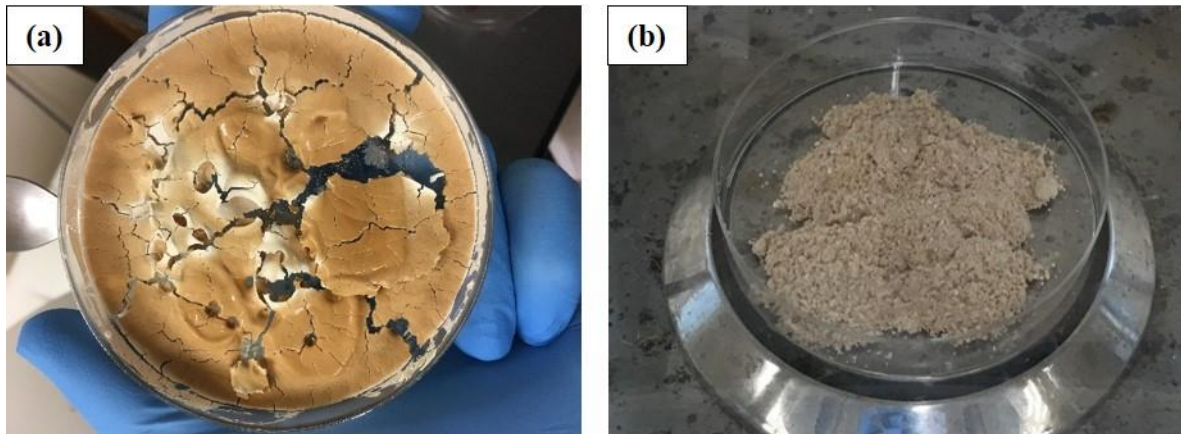


Figure 10: Bacteria spores: (a) dried using freeze-dryer machine; (b) crushed using ball mill.

### 3.2.2 Synthesis and microencapsulation

In this study, molar ratio of 1.2 M MDI (NCO 15.5%) to 1 M Jeffamine D230 was used (chain extender). based on the manufacturer (vendor) fact sheet and the calculations shown below, the equivalent weight (E.W.) of MDI (NCO 15.5%) and Jeffamine D230 were 271.097 and 120, respectively.

$$\text{E.W of MDI (NCO 15.5\%)} = \frac{\text{N+C+O}}{15.5\%} = \frac{14.0067+12.0107+15.9994}{15.5\%} = 271.076$$

$$\text{E.W of Jeffamine D230} = 120$$

$$\frac{271.076}{120} = 2.26 \rightarrow \text{Using ratio of 1.2:1, 2.712 g MDI react with 1 g Jeffamine D230}$$

The hardness of the shell for capsules depends on the isocyanate index of system, which consequently can be used to adjust the brittleness of the capsules to a desired level. In order to have more flexible and brittle capsules, isocyanate index of 1.2:1 was used. The produced capsules exhibit flexibility that allows survival during mixing, yet processes adequate brittleness to allow rupture during crack formation. Bacteria and nutrition were encapsulated in polyurea microcapsules using the in situ polymerization technique. In situ polymerization is an interfacial polymerization. In this technique, just one single monomer, either water or oil soluble, is employed. The reaction occurs at the interface of the organic and water phases at elevated temperatures and with the aid of a catalyst [129].

In this approach, 8.7 g Jeffamine D230 was mixed with 3.75 g span 85 in 150 ml acetone in a beaker using a mechanical mixer for 15 min at 400 rpm in room temperature prior to the addition of polymerization reactor. The solution was subsequently transferred to the reactor. The temperature in the reactor was adjusted at a relatively high temperature of 52 °C to accelerate the curing reaction. The bacterial spore powder (2.29 g), calcium lactate (20 g) and LB (5 g) were mixed with distilled water (15 g) in a beaker for 30 seconds using a spatula. MDI (23.6 g) was added by syringe to the paste and mixed for another 30 seconds. The paste was poured into syringe and injected slowly into the reactor and mixed for 2 hours at 400 rpm and 52 °C. The mixing speed was reduced to 200 rpm and 200 ml hot distilled water (52 °C) was added before mixing was continued for another 2 hours. Microcapsules (EPU) were washed by hot water during the filtration process using a vacuum pump and a Buchner funnel. Finally, they were dried in oven for 3 hours at 70 °C (Figure 11). Figure 12 schematically depicts the process of synthesis and encapsulation of bacteria in polyurea capsules using in situ polymerization method.



Figure 11: Filtration and oven drying of microcapsules (EPU)

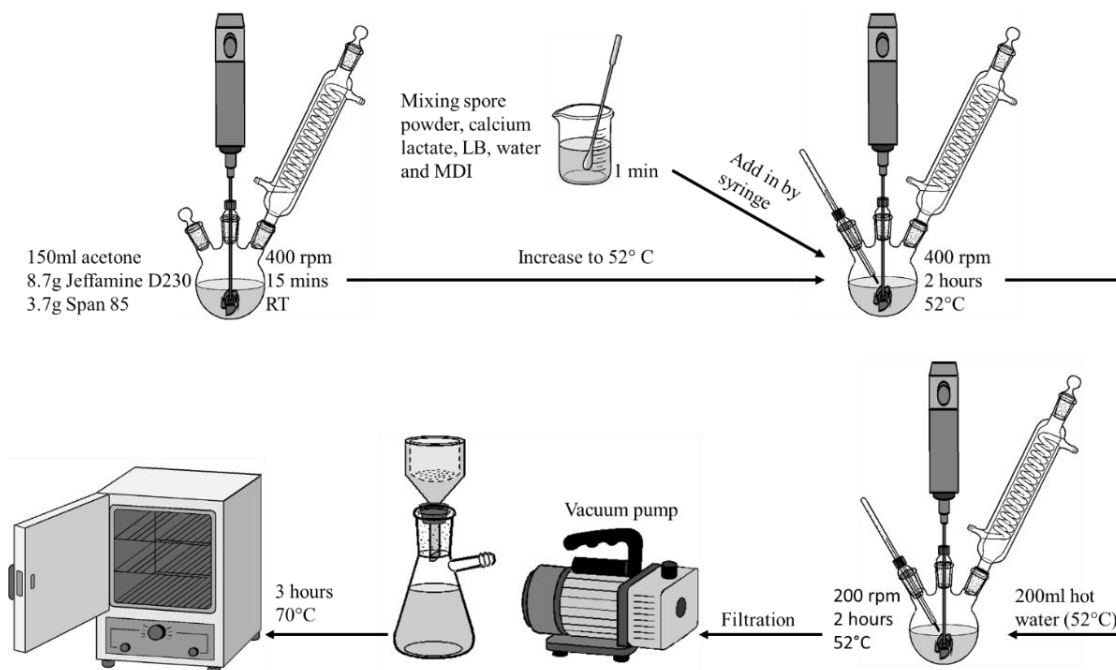


Figure 12: schematic illustration of synthesizing and encapsulation of bacteria in polyurea capsule.

### 3.2.3 Material preparation to investigate encapsulation

It is instrumental to ensure successful encapsulation of the core material and spores (Figure 13a) ability to germinate and consume the available calcium source to initiate calcium carbonate precipitation. For this purpose, 10 g of microcapsules were ball-milled in a container rotating at 300 rpm for 2 min (Figure 13 b and c). Then, 4 g of powdered microcapsules comprised of bacterial spore, polyurea capsules, calcium lactate and LB are introduced into two separated Erlenmeyer flasks filled with LB (M1) and distilled water (M2) as growth media (Figure 13d). The flasks were aerobically incubated at 37 °C and stirred at 150 rpm for 8 day [130]. The optical density (OD 600 nm) was measured at elapsed times of 0 h, 24 h and 48 h to confirm germination of the bacteria. A standard microscopic technique was used to observe bacterial growth after 24 h and 48 h of incubation. At the end of the eighth day, the solutions in each Erlenmeyer flasks were washed with water and ethanol by repeated centrifugation at 7000 rpm for 3 min to eliminate the growth media residue and cellular debris. The obtained solid material was oven dried for 5 hours at 70 °C. The washing and centrifuging solid particle

with water is meant to remove any calcium lactate (soluble in water) and keep the calcium carbonate (insoluble in water). The removal of calcium lactate allows further testing to confirm the presence of the calcium only in the calcium carbonate form.

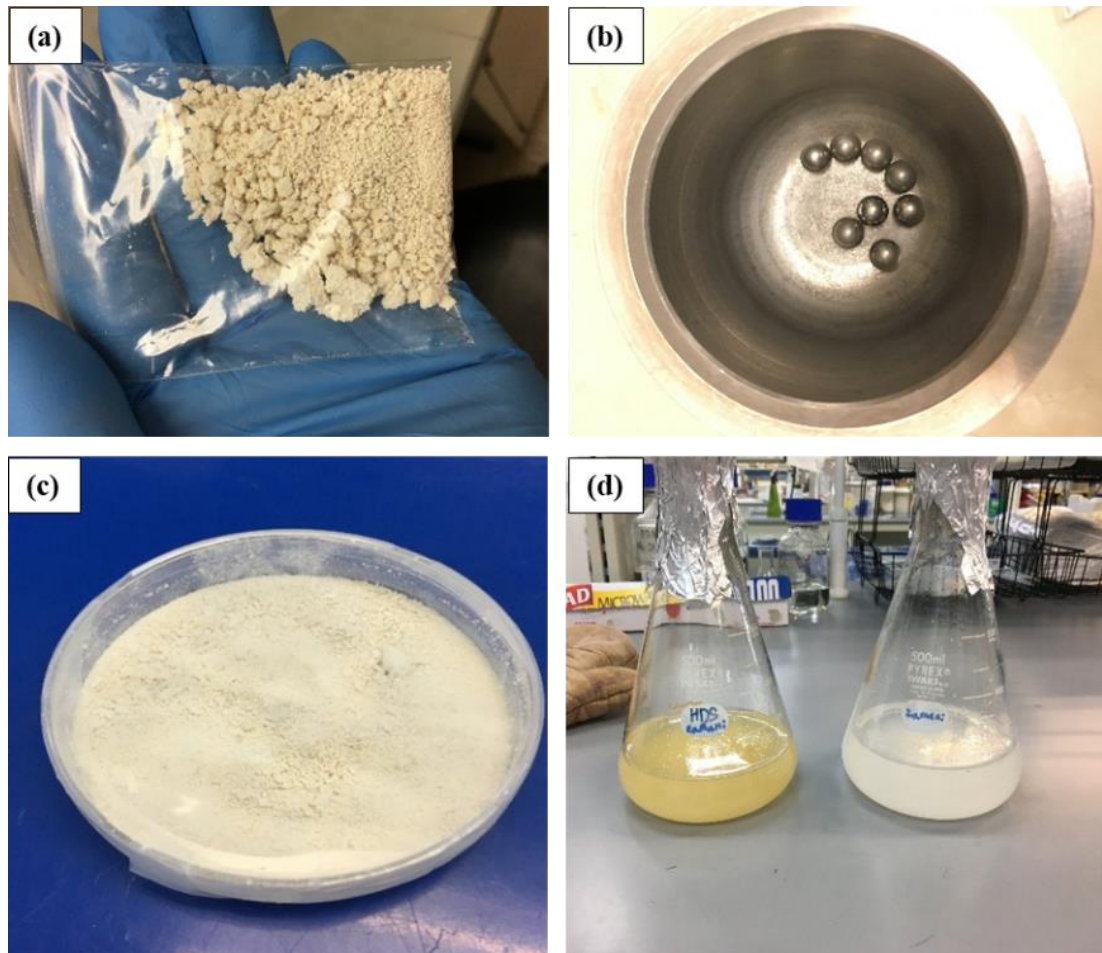


Figure 13: Material preparation for investigation of encapsulation and calcium carbonate precipitation: (a) synthesized microcapsules; (b) ball bearings for crushing microcapsules; (c) powder of crushed microcapsules; (d) pouring crushed microcapsules in flasks of water and LB.

### 3.2.4 Preparation of cement paste specimens

Cement paste specimens were prepared using ordinary portland cement (ASTM C150 Type I 42.5, Tasek Corporation Berhad) and w/c of 0.4 to provide adequate paste flow to mix capsules. The microcapsules were well mixed and poured at the middle of prism during casting the cement paste into  $25 \times 25 \times 100$  mm steel molds. A 2 mm-thick aluminum plate was inserted into the cast specimen to create a notch. The samples were unmolded carefully 1 day after

casting and immersed in water for curing at room temperature for 7 days before the creation of the artificial crack (Figure 14).



Figure 14: Casting of cement paste specimens with the artificial notch.

At the end of 7 days curing, specimens were artificially cracked using universal testing machine. A loading rate of 0.05 mm/min was applied until a visible crack is created on the bottom surface of the specimens (Figure 15). Then, the cracked sample was immersed in water again for 3 days. The aqueous environment triggers the encapsulated spores for germination. The image of cracked area in samples were subsequently recorded before and after healing for comparison. Dino Lite (AM4113/AD4113) microscope was used for this purpose.

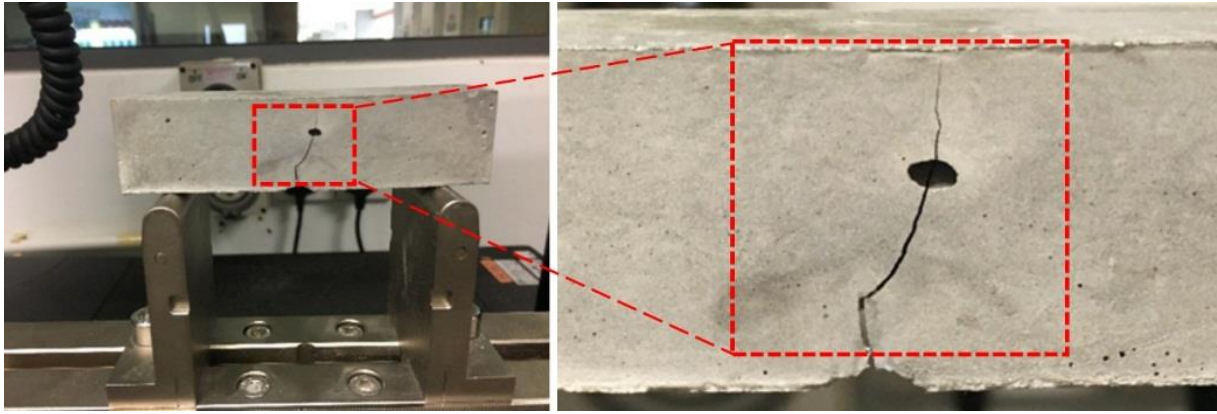


Figure 15: Crack creation using three point bending method

### 3.3 Characterization Tools

#### 3.3.1 Chemical

**X-ray powder diffraction (XRD)** – The mineralogy and crystallinity of the precipitates and microcapsules were determined by using XRD diffractometer (XRD, D8 Discover Bruker) with  $\text{CuK}\alpha 1$  radiation ( $\lambda=1.54060 \text{ \AA}$ ) in the  $2\theta$  range between  $10^\circ$  and  $90^\circ$  and a step size of  $0.02^\circ/\text{s}$ . Bragg- Brentano beam method was used at 40 kV and 40 mA to detect the presence of crystalline phases in samples.

**Energy-dispersive spectroscopy (EDX)** – Energy-Dispersive X-Ray (Oxford Horiba Inca XMax50) analysis was used to identify and confirm the presence of calcium in microcapsules (calcium lactate), nature of the produced calcium carbonate and elemental analysis of microcapsules (by point). The equipment was attached to the FE-SEM to allow for elemental information of the sample.

**Fourier transform infrared spectroscopy (FTIR)** – Fourier transform infrared spectroscopy (FTIR) was used to analyse the functional groups in polyurea microcapsules, calcium carbonate in crushed microcapsules and cement paste samples. The attenuated total reflectance (ATR) method was applied in generating the FTIR of the samples. The obtained spectrum was developed using an average of 64 scans from  $500 \text{ cm}^{-1}$  to  $4000 \text{ cm}^{-1}$  at a resolution of  $4 \text{ cm}^{-1}$ .

Raman Spectroscopy – Raman spectroscopy is a spectroscopic technique applied to identify molecules and study chemical bonding of polyurea microcapsules. The samples were analyzed using IR 785 nm at range between 670-730  $\text{cm}^{-1}$  and 150-180  $\text{cm}^{-1}$ .

### **3.3.2 Thermal tests**

**Thermogravimetric analysis (TGA)** – The measured weight loss curve in TGA indicates the changes in sample composition associated with elevating the temperature and subsequently evaluates its thermal stability. Also, a derivative weight loss (DTA) curve can show the point (temperature) at which the weight loss is most apparent. A thermogravimetric analyser (TGA, Q50) was used to study the thermal decomposition behaviour of the microcapsules, the detection of the calcium lactate and calcium carbonate at temperature ranging from 30 °C to 800 °C with a heating rate of 20 °C /min using nitrogen flow of 40 ml/min.

**Differential scanning calorimetry (DSC)** – In this study, DSC was used to measure the glass transition temperature ( $T_g$ ) of polymeric capsules. Microcapsule samples were analyzed using single and double scan method at temperature ranging from -50 °C to +150 °C with a heating rate of 10 °C/min under nitrogen flow of 40 ml/min.

### **3.3.3 Microstructural**

Field emission scanning electron microscope (FE-SEM) – The morphology of microcapsules, bacterial precipitated calcium carbonate and cement paste were analysed by the micrograph images obtained using FE-SEM (FESEM, SU8010 Hitachi) operating under 10 Kv voltage. The microcapsules and cement paste samples were coated with platinum for 40 seconds with a sputter current at 30 mA using a coater (Quarum Q150R S) prior to the analysis.

## **4. RESULTS AND DISCUSSION**

The microscopy technique was used to detect and confirm the growth of bacteria. The produced bacterial spore powder (healing agent) together with the nutrition were used as a core material

for encapsulation in polyurea microcapsules. OD600, light microscopy, TGA, FT-IR, XRD, FE-SEM and EDX were used to prove successful encapsulation of the core material in the synthesized microcapsules. The synthesized microcapsules were characterized by FT-IR, Raman, XRD, AFM, DSC, FE-SEM and EDX. Finally, the microcapsules were added to the cement paste mix and triggered to prove self-healing. Dino lite microscope, TGA, XRD, FE-SEM and EDX techniques were used for this purpose. The following describes the process of bacterial spores preparation, synthesis and encapsulation of bacterial spores in polyurea and proof of self-healing of concrete using the designed capsules.

#### 4.1 Bacteria Viability and Growth

Viability and quantification of bacterial growth was done by serial dilution and plating on supplemented LB agar. Viability experiments were conducted in triplicates to establish statistical confidence. One hundred (100)  $\mu\text{l}$  of the bacterial culture was sequentially transferred into 900  $\mu\text{l}$  of LB medium for a total of 9 dilutions. Cells plated after the 6<sup>th</sup> dilution were countable. The plates obtained from spreading the 7<sup>th</sup> dilution were chosen for quantification (Table 5 and Figure 16).

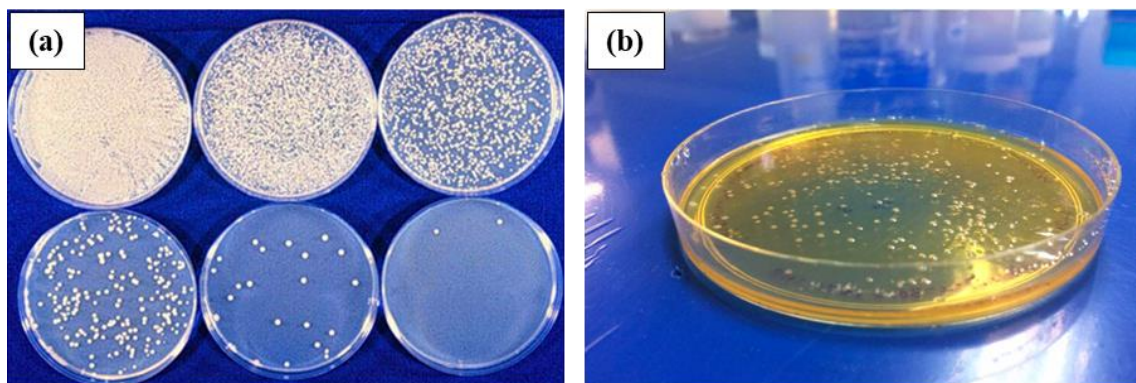


Figure 16: Single colonies obtained from serial dilution of bacteria in LB medium: (a) Typical dilution results showing lawn (uncountable) growth diluted to manageable counts (Photo courtesy of Kansas State University department of physics); (b) colonies observed on the plate obtained from our 7<sup>th</sup> dilution.

Table 5: Viability of *B. pseudofirmus* during culture and sporulation

Phase	Incubation <sup>a</sup>	Avg ABS (600nm) <sup>b</sup> - $\sigma^c$	Avg colonies ( $\times 10^7$ ) <sup>b</sup> - $\sigma$	CFU/ml ( $\times 10^9$ )	Efficiency (%)
Initial viability	48 hours	1.997 – 1.952	172.67 – 21.64	1.73	N/A

Sporulation	96 hours	2.087 – 2.077	253.67 – 30.13	2.54	N/A
Post sporulation (Initial)	5 day	1.504 – 1.450	158.00 – 19.82	1.58	91
Post sporulation (powder)	15 day	1.522 – 1.539	157.67 – 14.52	1.58	91

<sup>a</sup> Post inoculation

<sup>b</sup> Triplicate trials were attempted

<sup>c</sup>  $\sigma$  standard deviation

## 4.2 Synthesis and Microencapsulation of Bacteria and Nutrition

In this section, the process of synthesizing the polyurea microcapsules are discussed. The bacteria and calcium lactate (core material) were encapsulated in polyurea using in situ polymerization technique (EPU). The oven-dried microcapsules (shown in Figure 17) were characterized using various destructive and non-destructive techniques, as will be discussed.



Figure 17: Synthesized polyurea microcapsules using bacteria, calcium lactate and LB as core material

### 4.2.1 Chemical characterization

**FT-IR Spectroscopy** – FT-IR spectroscopy was performed on EPU microcapsules and the materials used in the encapsulation of bacterial spores (**Error! Reference source not found.**).

The spectrum for MDI (NCO 15.5%) indicates two absorption bands at wave numbers of 2970  $\text{cm}^{-1}$  and 2868  $\text{cm}^{-1}$ , signifying the aliphatic C–H stretching vibrations of methyl and methylene groups, respectively [131]. The sharp and strong absorption peak at 2255  $\text{cm}^{-1}$  is attributed to the presence of the isocyanate groups (N=C=O). The spectrum of MDI also signified sharp peaks at 1522, 1608 and 1727  $\text{cm}^{-1}$ , which are indicative of C=C stretching of the aromatic ring [132]. Also, the peaks at 2868 and 2966  $\text{cm}^{-1}$  in Jeffamine D230, at 2852 and 2950  $\text{cm}^{-1}$  in span

85 and at  $2980\text{ cm}^{-1}$  in calcium lactate are assigned to C-H stretch (alkane). The peaks at  $1100\text{ cm}^{-1}$  in MDI and jeffamine,  $1119\text{ cm}^{-1}$  in calcium lactate and  $1094\text{ cm}^{-1}$  in EPU are attributed to C-O stretching. There is a broad and strong peak in the FT-IR spectrum of the calcium lactate at  $3150\text{ cm}^{-1}$  that can be associated with the hydroxyl groups [133]. FT-IR spectrum of synthesized polyurea shows that the NCO peak at  $2255\text{ cm}^{-1}$  has completely disappeared, meanwhile urea bond N-H stretching peaks at  $3324$  and  $1541\text{ cm}^{-1}$  were observed. These observations indicate successful synthesis of the polyurea polymer structure [134].

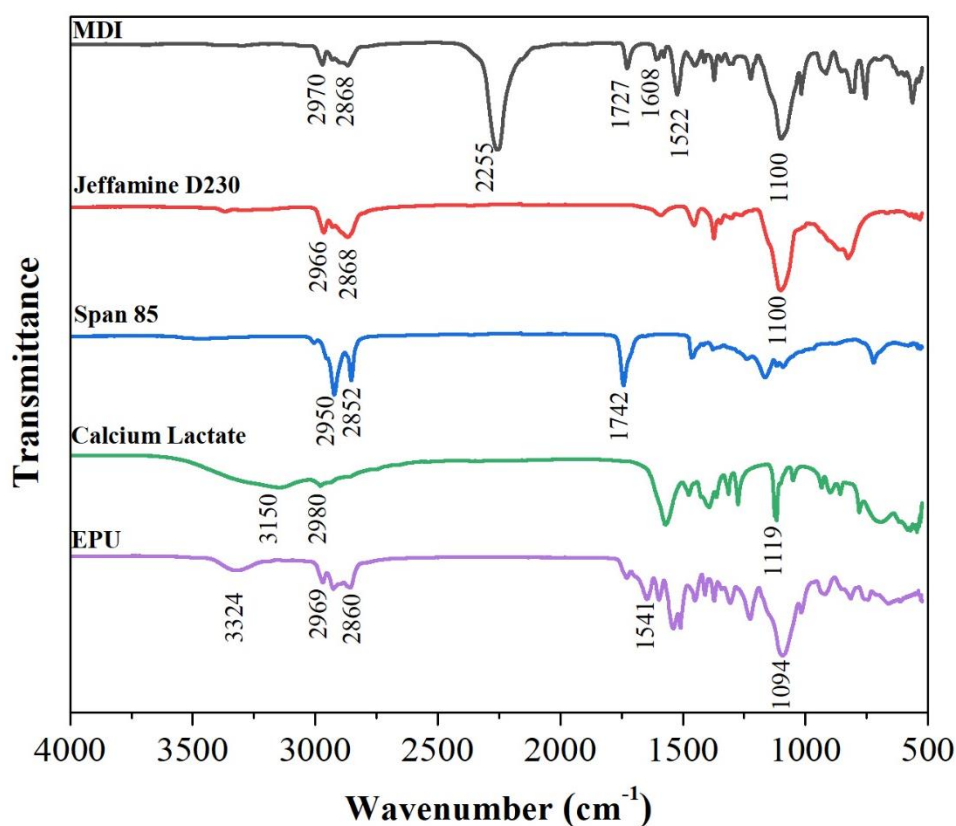


Figure 18: FT-IR spectra of the encapsulated bacteria, calcium lactate and LB in polyurea microcapsules.

**Raman** – Chemical bonding and molecules identification were analysed using the Raman spectroscopy technique (Figure 19). The strong bond at  $410\text{ cm}^{-1}$  is related to the polyurea structure. It confirms the presence of the urea linkages in both pure state and encapsulated calcium lactate in polyurea capsules [135]. There is an active bond at a wave number of about  $790\text{ cm}^{-1}$  observed only for calcium lactate in the polyurea capsules. This bond distinguishes

the calcium lactate. Another bond is observed at wavenumber of  $711\text{ cm}^{-1}$  which is related to calcium lactate. Both peaks confirm the successful encapsulation of the calcium lactate in the polyurea capsules [136].

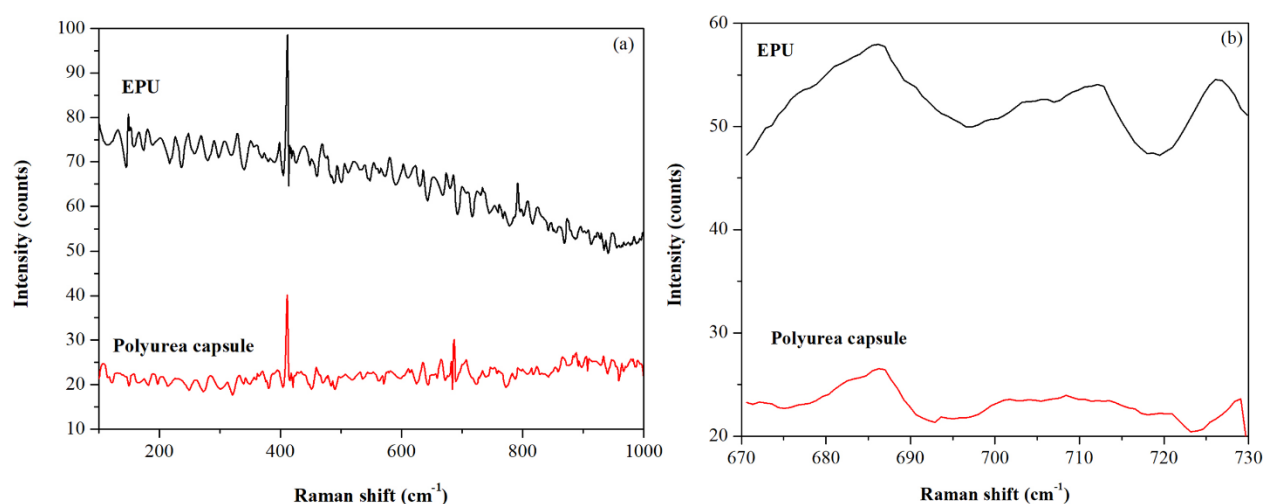


Figure 19: Raman spectra of EPU and pure polyurea capsule with Raman shifts (a) 0 to  $1000\text{ cm}^{-1}$ ; and (b)  $670\text{ cm}^{-1}$  to  $730\text{ cm}^{-1}$ .

**XRD** – The semi-crystalline structure of the polyurea is observed as peak intensities in the region  $10^\circ < 2\theta < 30^\circ$  of the XRD signature (Figure 20). With the several peaks observed in this region, it is interfered that the synthesized polyurea is not amorphous, but rather semi-crystalline. The chemical structure of the polyurea is based on C-H, C-O and C-N bonds [137, 138]. As such, the peaks are not too sharp but rather wide. Crystalline domains with strong hydrogen bonds are formed by the urea motifs, while the amorphous domains was formed by carbon chains. Therefore, increase of carbon chain length together with increase amorphous domains lead to decrease the crystallinity [139]. Unlike XRD pattern for PU capsules, a peak was found at  $2\theta$  of  $42^\circ$  for synthesized polyurea. Since calcium lactate was loaded in the synthesized polyurea microparticles, it can be concluded that the peaks are indicative of calcium lactate [140, 141].

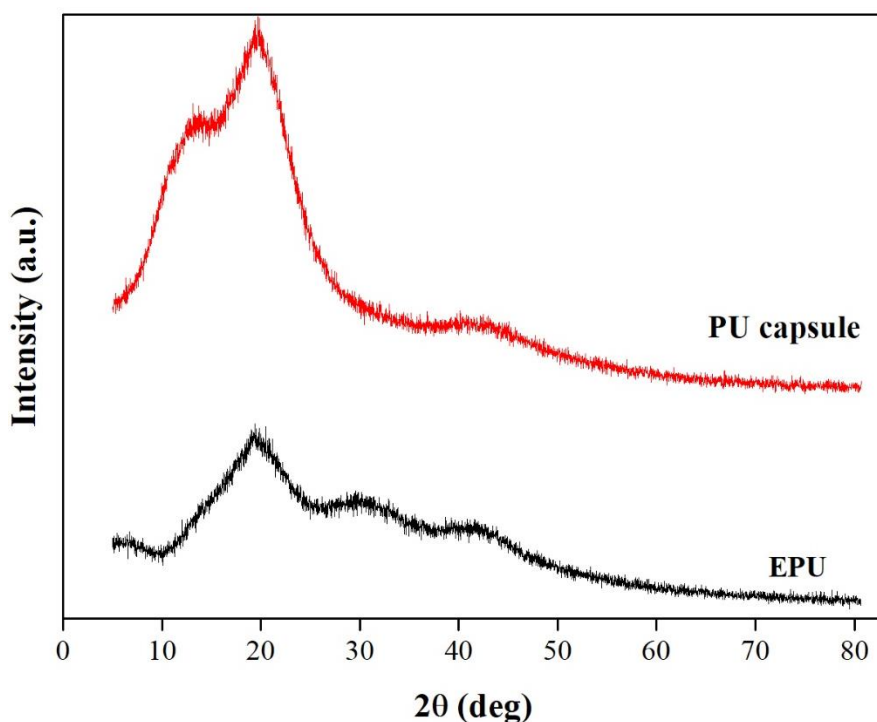


Figure 20: XRD patterns of EPU and polyurea capsule

#### 4.2.2 Thermal analysis

**TGA** – Thermogravimetric analysis was carried out to study the thermal stability and loading of the calcium lactate in the synthesized microcapsule. TGA/DTA of samples are shown in Figure 21. The respective details of TGA are presented in Table 6. The thermal stability of the calcium lactate is much lower than that of the polyurea, as suggested by the lower values of  $T_{5\%}$ ,  $T_{50\%}$ ,  $T_{char}$  and  $T_{max}$  of the calcium lactate. For instance, 5% of PU microcapsules, EPU and calcium lactate were degraded at the temperature of 284.5 °C, 272.7 °C and 76.1 °C, respectively. The difference between PU microcapsules and EPU is the presence of calcium lactate in EPU. Since calcium lactate has lower thermal stability comparing to PU microcapsules, thus EPU with encapsulated calcium lactate is expected to have lower thermal stability.

Table 6: Thermal stability characterization of synthesized microcapsules and calcium lactate

Sample ID	$T_{5\%}$ <sup>a</sup> (°C)	$T_{50\%}$ (°C)	$T_{char}$ (°C)	Wt loss (%)	$T_{max}$ (°C)
PU microcapsules	284.5	374.7	791.26	95.72	401.88
EPU	272.7	355.4	791.29	97.15	407.16
Calcium lactate	76.1	426	791.12	79.9	100.55

<sup>a</sup>:  $T_{5\%}$  represents that 5% of sample degraded at that temperature

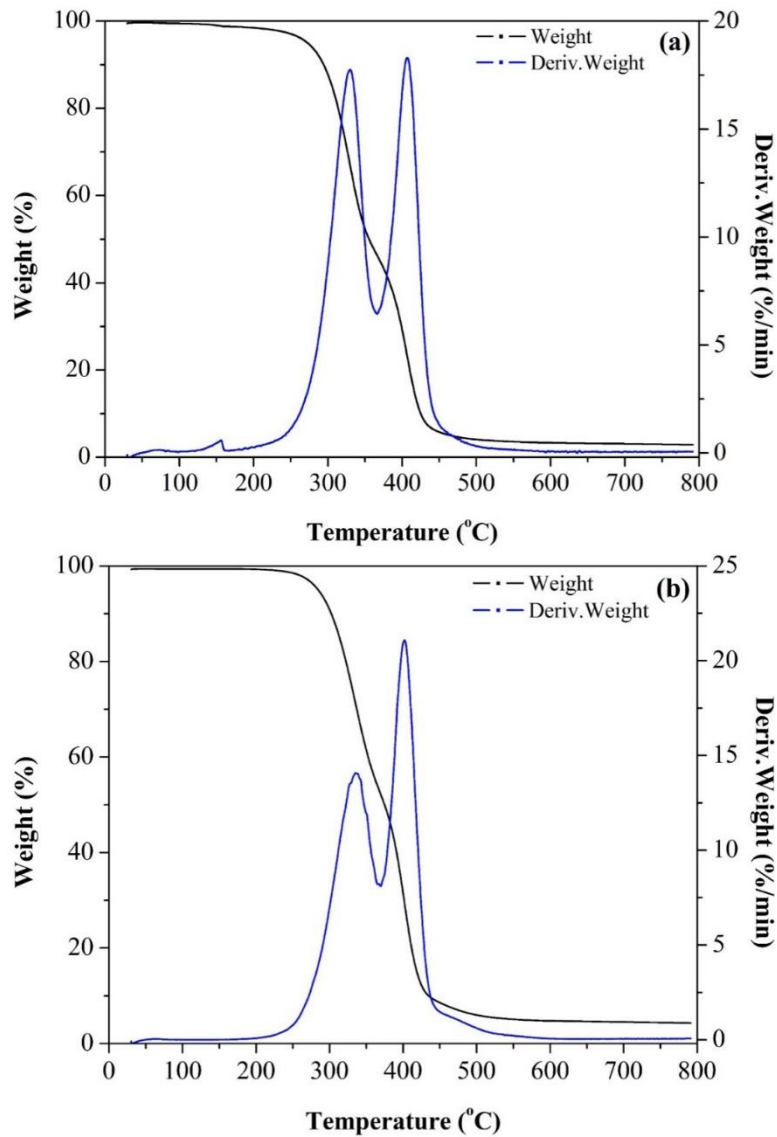


Figure 21: Thermal analysis of: (a) EPU, microencapsulated bacteria and calcium lactate in polyurea capsule; (b) polyurea microcapsules.

**Differential scanning calorimetry (DSC)** – Glass transition of the encapsulated bacteria and the calcium lactate in the polyurea capsules (EPU) and the pure polyurea capsule (PU) were determined using DSC (Figure 22). The  $T_g$  of the pure polyurea is  $-12\text{ }^\circ\text{C}$ , indicating high flexibility at room temperature. It is observed that  $T_g$  of the capsules without the calcium lactate is significantly lower than that of the capsules with calcium lactate ( $5\text{ }^\circ\text{C}$ ). This difference is expected. The presence of the calcium lactate in the capsules significantly increases  $T_g$  of the capsules due to the former's high  $T_g$ .

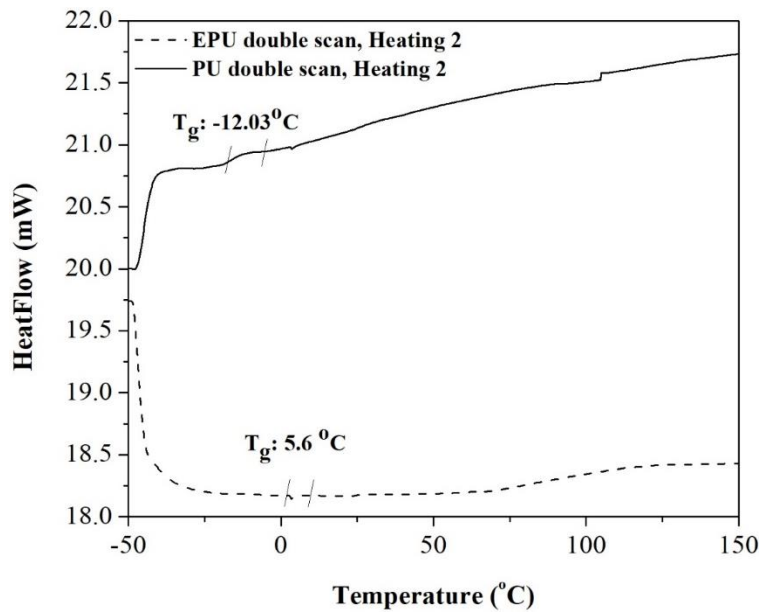


Figure 22: Thermograms of EPU and pure polyurea capsules using second heating rate

#### 4.2.3 Microstructural analysis

FE-SEM was used to study the morphology and size distribution of the synthesized microcapsules. Figure 23 shows the synthesized microencapsulated bacteria and the nutrition in polyurea capsules. FE-SEM was used to measure the sizes of 270 synthesized capsules. The capsule sizes vary from 0.2 mm to 1.3 mm, with approximately 57% of the capsules ranging from 0.3 to 0.6 mm.

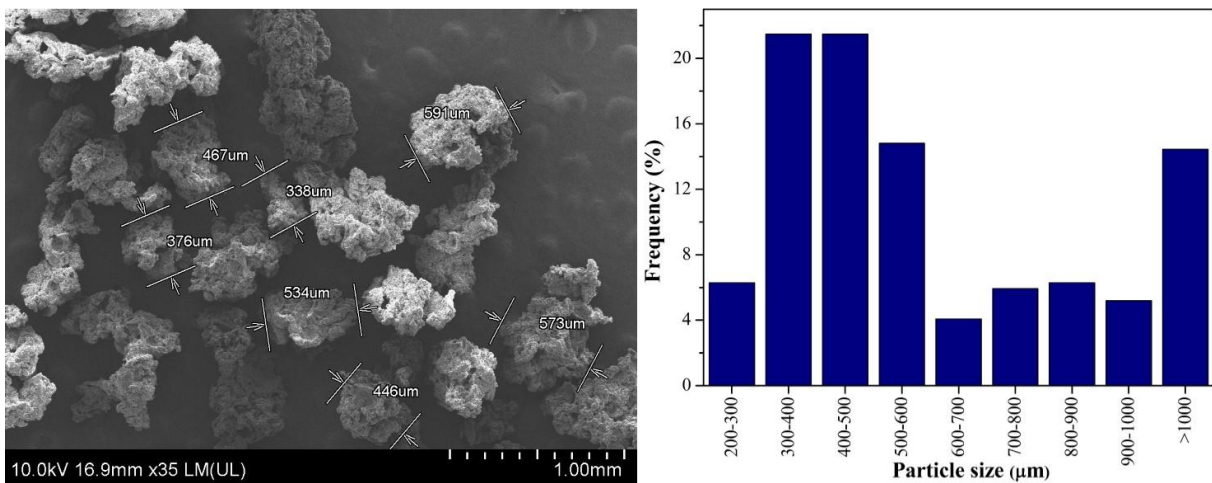


Figure 23: Size distribution of synthesized microencapsulated bacteria and calcium lactate in polyurea capsules (frequency is expressed as a percentage of particles falling within each size range).

Synthesized microcapsules have irregular shapes with rough surfaces, which allow good bonding with the cementitious matrix. The shape and surface of the polyurea capsule (without the core material) are very similar to EPU. This proves that encapsulation of bacteria and nutrition in polyurea capsules did not affect the morphology of the microcapsules. Figure 24 depicts the morphology of the capsules at different magnification. Polyurea capsule has irregular shape with non-uniform surface which is similar to synthesized capsules in EPU. The microimages show that the surface of microcapsules has many protrusions and holes, which may have occurred due to the release of CO<sub>2</sub> during the reaction of isocyanate with water (as expressed in Equation 4).

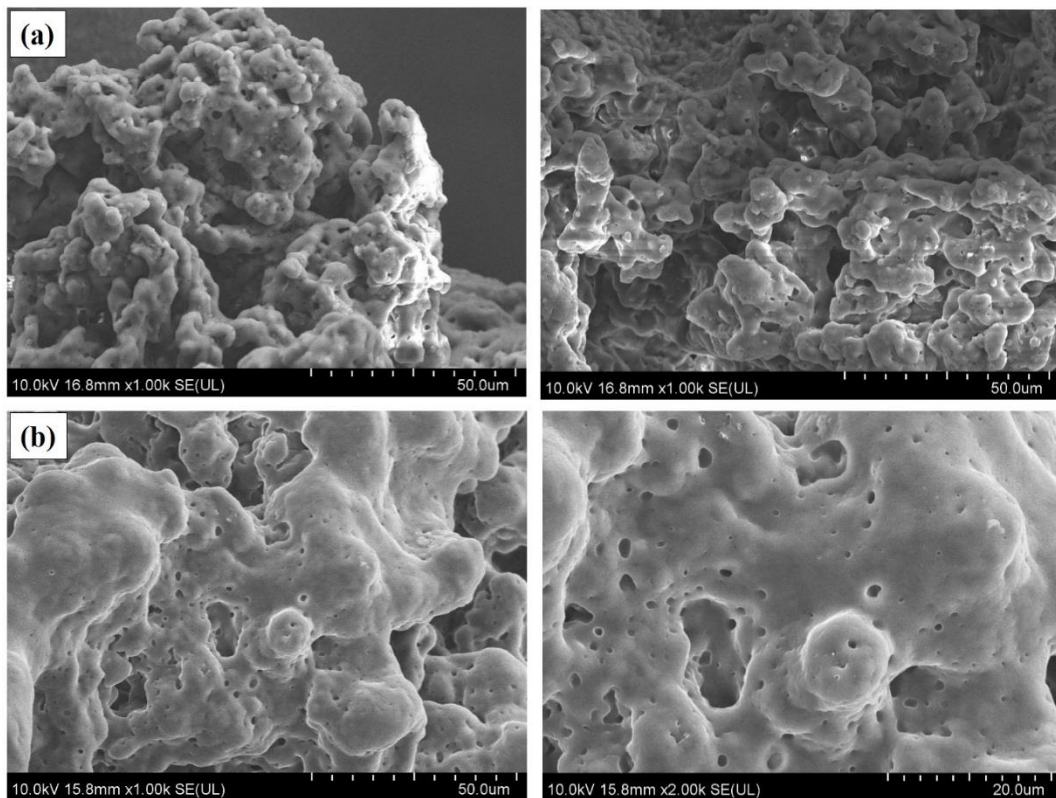


Figure 24: Synthesized microcapsules have irregular shapes with many protrusions and holes due to release of CO<sub>2</sub>: (a) EPU; (b) pure polyurea capsule.

EDX analysis was performed to confirm the presence of the calcium lactate in the capsules.

The microimage in Figure 25a shows the elements of the virgin polyurea capsules (carbon,

nitrogen and oxygen). Figure 25b shows the polyurea capsule with the calcium lactate. The detected calcium confirms loading (presence) of the calcium lactate in our capsules. In addition, the amount of oxygen in EDX of capsules with the calcium lactate is higher than that in the pure polyurea (22.7% to 17.6%). This is attributed to the presence of higher oxygen content (6 atoms) in the chemical structure of the calcium lactate. Therefore, adding calcium lactate has significantly increased the oxygen content.

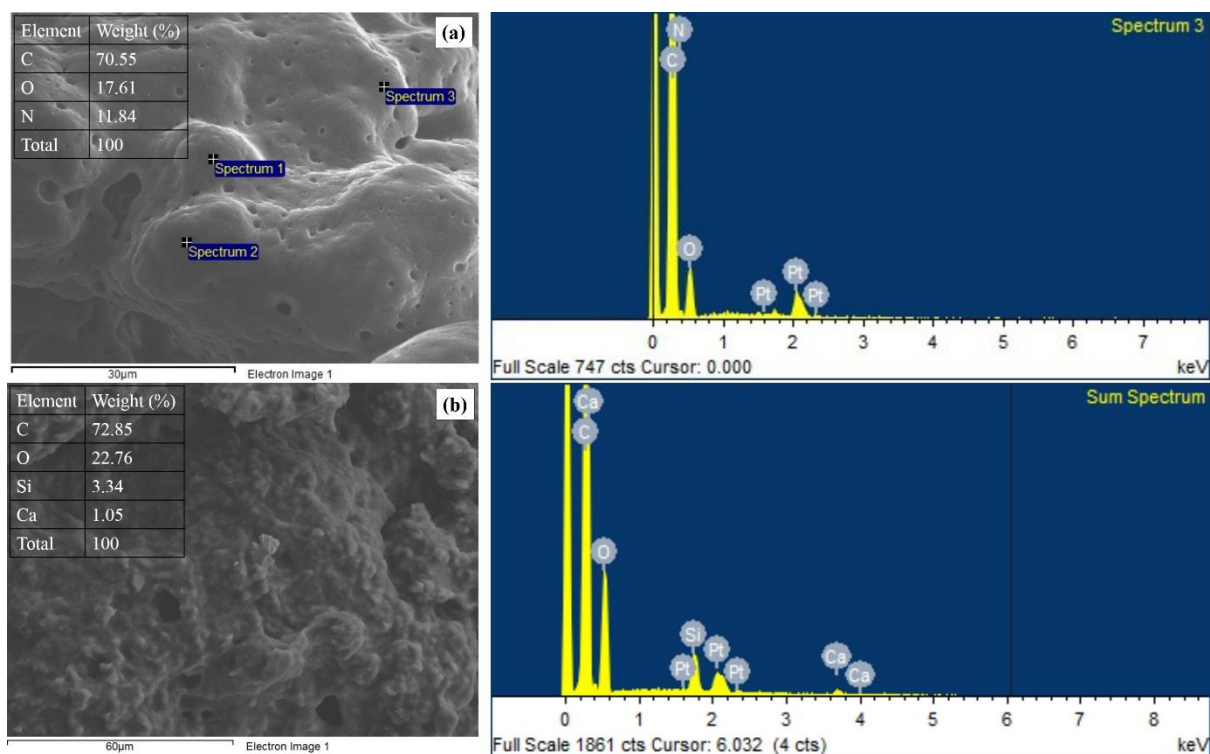


Figure 25: EDX analysis which confirms the presence of calcium lactate: (a) EPU; (b) pure polyurea.

### 4.3 Proof of Successful Bacterial Germination

Spectrophotometry is routinely used to estimate germination of bacteria by measuring the optical density (OD) of sample at a wavelength of 600 nm – designated as OD<sub>600</sub>. For this purpose, 1.0 ml volume of each samples was poured in cuvette using a pipette (Figure 26). OD<sub>600</sub> of *B. pseudofirmus* samples were measured at 0, 24 and 48 hours of incubation. A summary of the measurements are shown in Table 7. Pure distilled water and/or LB broth were used as a reference for each of the OD<sub>600</sub> measurements. The noticeable increases in the

measured OD<sub>600</sub> demonstrate that the crushed capsules contained spores and their capability of germination can be warranted. The OD<sub>600</sub> LB broth inoculated with *B. pseudofirmus* capsules increased from a reference value of 0.223 nm at 0 hour to 2.508 nm after 48 hours of incubation. However, the OD<sub>600</sub> measurement of the liquid from the flask containing water did not show any changes. The germination of *B. pseudofirmus* as a reference image is shown in Figure 27a. Figure 27b and Figure 27 c-d are showing the germination of bacteria after 24 h incubation in M1 (LB) and M2 (water), respectively. The concentration of bacteria was greater in M1 compared to M2, since there is a large amount of the nutrition available for bacterial growth in LB broth.

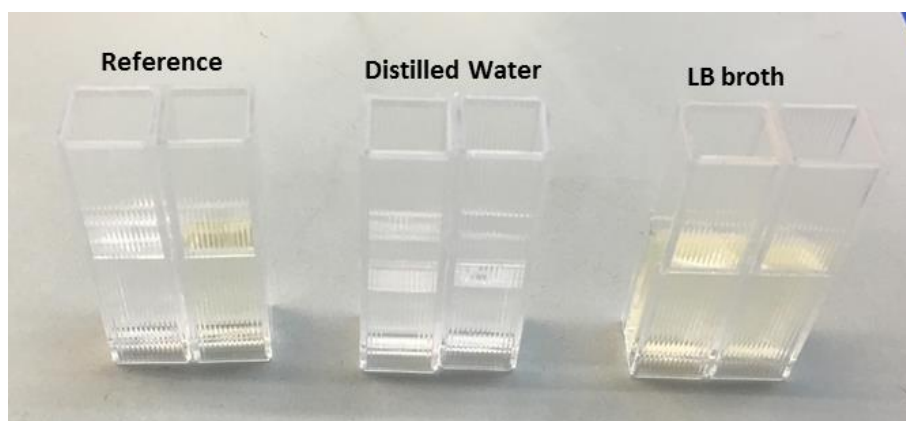


Figure 26: Preparation of samples for optical density measurement.

Table 7: OD<sub>600</sub> measurement results after 0, 24 and 48 h of incubation

<b>Solution</b>	<b>Time (h)</b>	<b>Blank, OD 600 (nm)</b>	<b>Capsule 1, OD 600 (nm)</b>	<b>Capsule 2, OD 600 (nm)</b>
Distilled water	0	0.046	0.166	0.123
	24	-	0.125	0.122
	48	0.045	0.087	0.084
LB broth	0	0.061	0.223	0.202
	24	-	2.06	2.078
	48	0.055	2.508	2.491

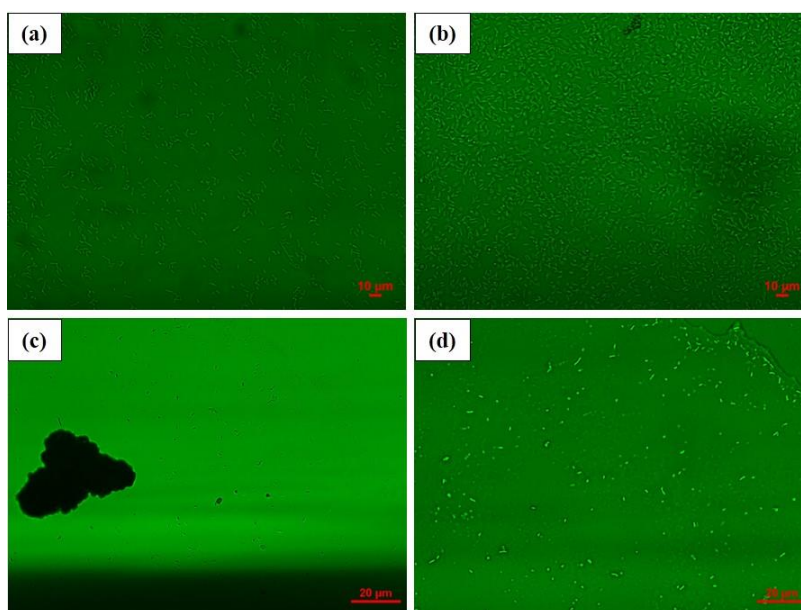


Figure 27: Images from fluorescence microscope: (a) *Bacillus Pseudofirmus* DSMZ 8715 spores; (b) bacterial spores germinated in M1 (LB) after 24 h; (c); (d) bacteria spores germinated in M2 (water) after 24 h

#### 4.4 Proof of Successful Calcium Carbonate Precipitation

**TGA** – Thermogravimetric analysis was performed for EPU, calcium lactate, calcium carbonate, crushed capsules (as described in chapter 3) incubated in M1(LB) and M2(water) to confirm the precipitation of the calcium carbonate (Figure 28). Table 8 shows the results for weight loss of EPU, calcium lactate, calcium carbonate, and crushed capsules incubated in water and LB. After breakage of capsules (crushed capsules), bacterial spores become activated upon contact with water and oxygen. The activated bacteria accordingly metabolizes the calcium lactate to produce calcium carbonate.

Table 8: TGA weight loss for synthesized microcapsules and calcium lactate

Sample ID	T <sub>5%</sub> (°C)	T <sub>50%</sub> (°C)	T <sub>char</sub> (°C)	Wt loss (%)	T <sub>max</sub> (°C)
Batch 1	272.7	355.4	503.6	96	407.1
Calcium lactate	76.1	426	791.1	79.9	100.5
Calcium carbonate	643.8	791.3 <sup>a</sup>	791.3	44.5	713.7
Crushed EPU in water	273.4	359	595.0	96	399.1
Crushed EPU in LB	272.1	371.1	791.2	94.6	400.4

<sup>a</sup>: 44.5% of calcium carbonate was degraded at the temperature of 791.3 °C

TGA results confirm the precipitation of the calcium carbonate by the encapsulated bacteria and calcium lactate. The weight loss (%) of calcium carbonate at around 800 °C is 44.53%, while the weight loss of EPU is 96%. The weight loss of the crushed capsules placed in LB decreased to 94.68%. It can be inferred that the thermal stability of the samples was improved due to the precipitation of the calcium carbonate. This results also confirms the precipitation of calcium carbonate. For the crushed capsules of EPU in water, the weight loss does not change over 8 day of incubation [130]. This could be due to the fact that the bacteria in water needs more time to grow than it does in LB medium, as the latter accelerates germination and calcium carbonate precipitation of the bacteria. Therefore, sufficient incubation time of crushed EPU in water will result in precipitation of the calcium carbonate.

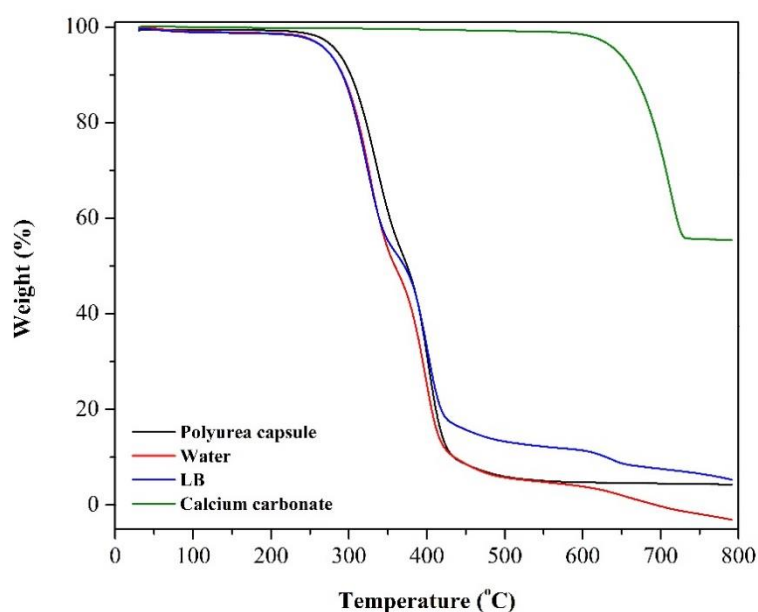


Figure 28: TGA graphs of pure polyurea capsule, crushed capsules incubated in water, LB and calcium carbonate

**FT-IR** – Fourier-Transform Infrared (FT-IR) spectra were obtained for the dried solid particles after 8 day of incubation in M1 (LB) and M2 (water). The FT-IR spectra shows precipitation of the polymorph calcium carbonate (calcite and vaterite) in both M1 and M2. The results compare well to the values reported in the literature [102, 142, 143]. The characteristic carbonate  $\nu_2$  band of calcite and vaterite is identified at a wave number of  $872\text{ cm}^{-1}$ , while the

carbonate  $\nu_4$  band of aragonite is spotted at wave number of  $713\text{ cm}^{-1}$  (Figure 29). The precipitation of calcium carbonate proves successful encapsulation of the bacterial spores and their nutrition in polyurea microcapsules.

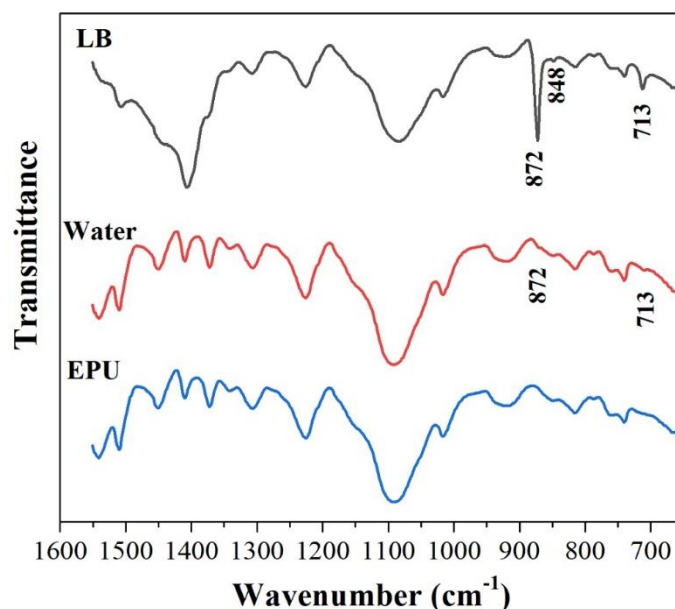


Figure 29: FT-IR spectra of the dried particles after 8 day incubation in water and LB

**XRD** – For further confirmation of the precipitation of the calcium carbonate crystal, XRD analyses were performed on the powder obtained from the crushed capsules after 8 day of incubation in water and LB. These particles were dried prior to performing the analysis. XRD diffraction spectra in Figure 30 shows precipitation of calcium carbonate. The peaks obtained at  $2\theta$  values of  $29.3^\circ$  (in water) and  $29.4^\circ$  (in LB) signify calcite as reported in the literature. The intensity of the peak at the  $2\theta$  value of  $29.3^\circ$  was higher in LB. As previously indicated, LB acts as an accelerator for bacteria germination; therefore, it increases the precipitation rate of the calcium carbonate. For this reason, the bacteria in LB produced more calcium carbonate after 8 day than that placed in water. These result collectively confirm the precipitation of calcium carbonate using bacteria and show good agreement with the results obtained from previous studies [80, 105, 144].

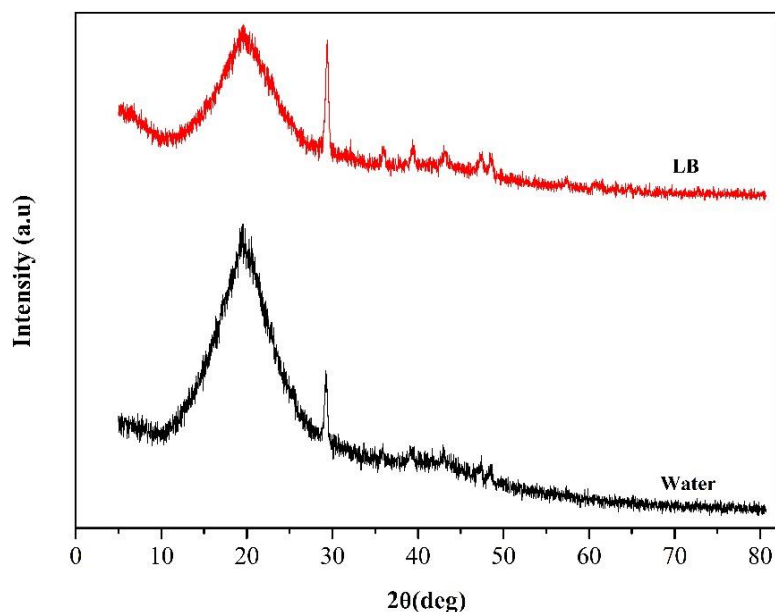


Figure 30: XRD spectra of dried particles obtained from incubation of crushed capsules in LB and water

**EDX** - EDX analysis was used to detect the calcium belonging to the calcium carbonate in dried particles obtained from crushed capsules in M1 (LB). EDX was conducted using the point technique in representative spots of the microimage (Figure 31). All samples were washed with water, centrifuged, and dried before analysis, in order to eliminate possible calcium lactate residues [143, 145]. The results confirm the detection of calcium element at peak 3.69 representing calcium carbonate.

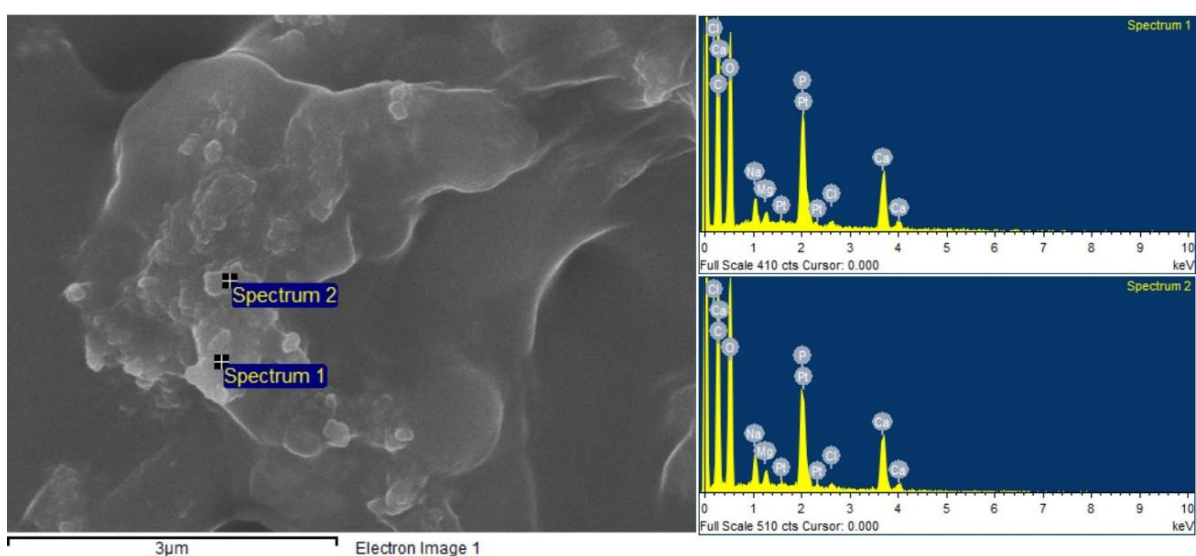


Figure 31: EDX analysis of dried solids by point analysis confirms precipitation of calcium carbonate

#### 4.5 Proof of Crack Healing

The cement paste specimens including healing capsules were artificially cracked using 3-point bending loading after 7 day of curing (Figure 32). The cracked samples were kept in water again. Upon creation of the crack, the embedded capsules rupture and the water activates the spores for germination. Precipitation of the white color particles (healing) was observed in the designated crack area after 3 day (Figure 33). The healed cracks were later analyzed using Dino-lite microscopy, FE-SEM and EDX to confirm precipitation of the calcium carbonate.

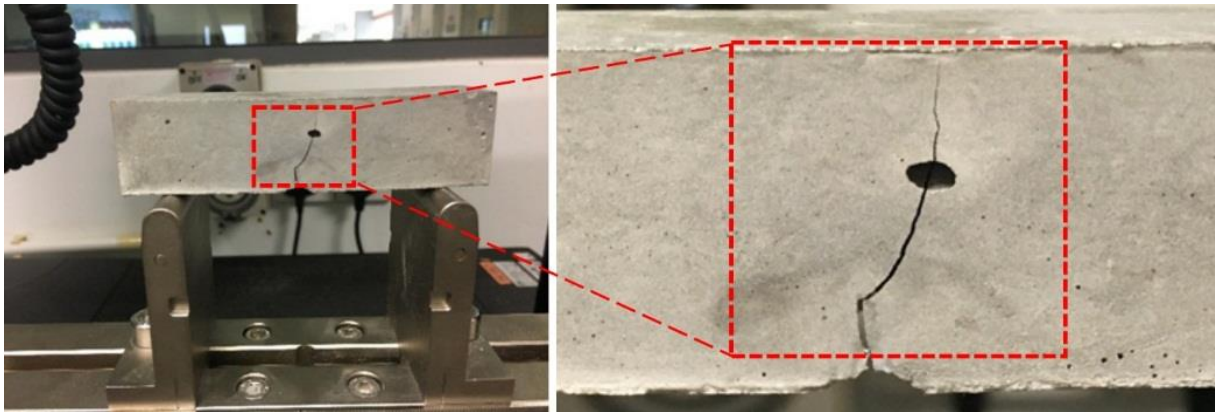


Figure 32: Crack creation using three-point bending/flexural test (after 7 day curing)

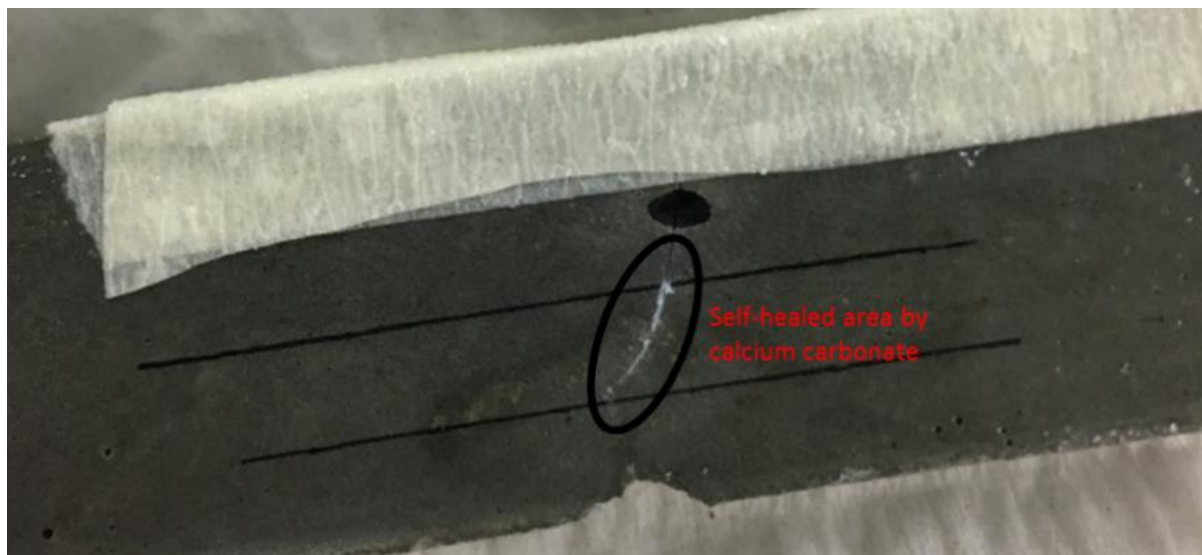


Figure 33: Crack healing of cement paste specimen as a result of the microbial precipitation of the calcium carbonate

##### 4.5.1 Crack healing tracking

Dino-lite microscope was used to observe the progress of healing in the designated crack section of the specimen before the microstructural analyzing. Figure 34 shows an image of a

crack in the specimen healed by calcium carbonate. A closer image with a magnification factor of 230X demonstrates the buildup of the healing product in the cracked area (Figure 34 b). This section of the specimen was used for FE-SEM, EDX and XRD to analyze and confirm the precipitation of calcium carbonate.

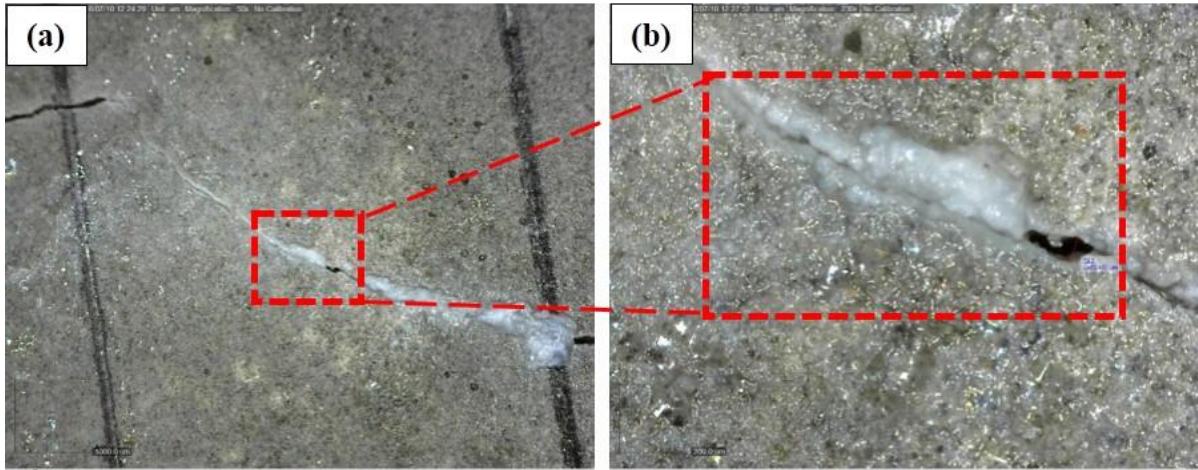


Figure 34: Dino Lite microscopy image of the crack filled with precipitation of calcium carbonate at magnification factors of: (a) 50X; (b) 230X.

#### 4.5.2 Microstructural analysis of precipitated calcium carbonate

**FE-SEM and EDX** – The precipitated material was analyzed using microstructural techniques to confirm the presence of the calcium carbonate. The morphology of the precipitated crystals were investigated at different magnification levels. The results from the literature suggest that the morphology and size of the crystals depend on many factors, such as the type of bacteria and their nutrition source [146]. As shown in Figure 35, the crystals have an amorphous structure and an irregular shape. Some of the crystals are formed by accumulation of platy crystals. The nature of the crystals were analyzed using point analysis for different areas at preselected magnifications. As depicted in Figure 36, EDX analysis results show a high peak for Ca element at 3.69 in all spectra. This proves that the crystals are calcium carbonate. The Ca element is not related to cement, because the morphology of cured cement is ettringite and needle-shaped as shown in Figure 37. Hence, it can be concluded that the white precipitated particles are solely related to the precipitated calcium carbonate.

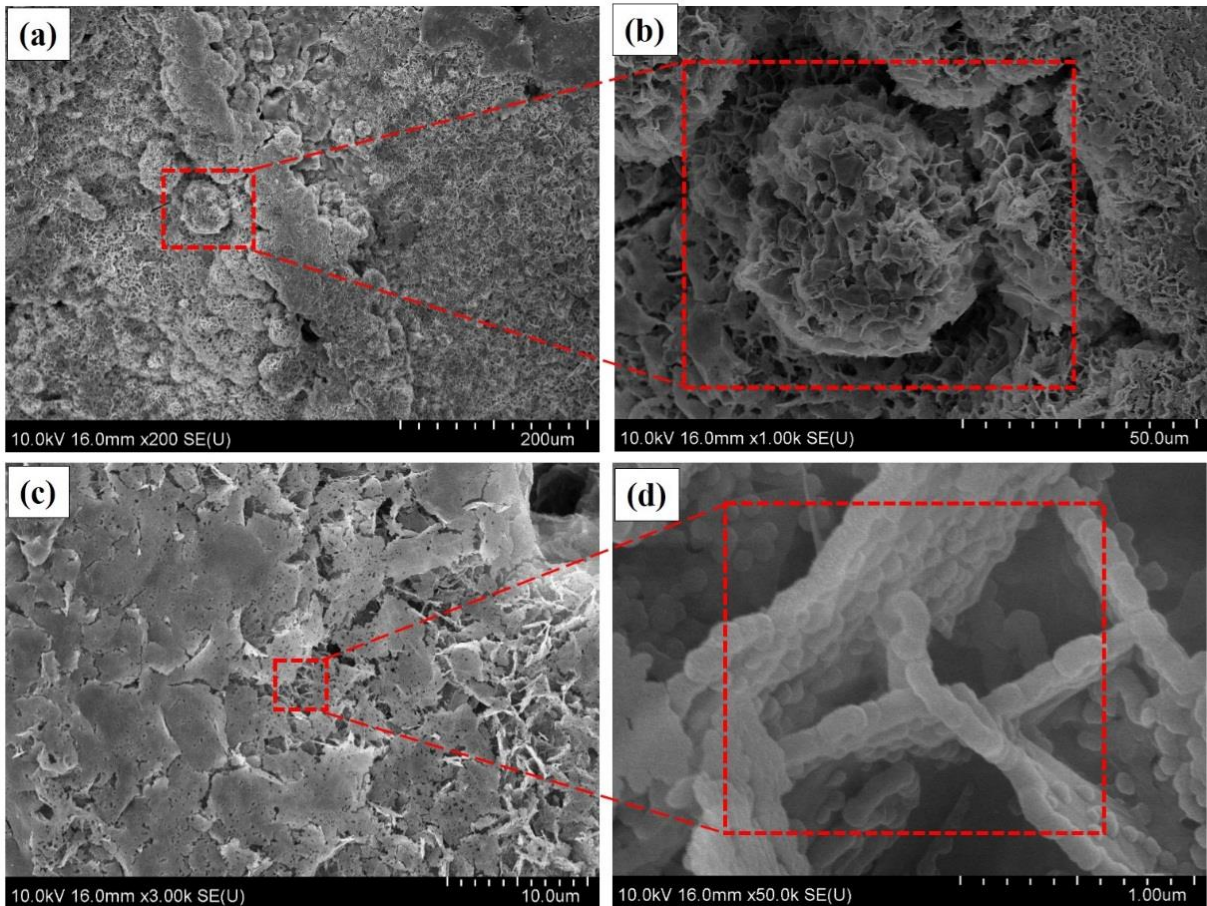


Figure 35: precipitated white particles which was analyzed by FE-SEM and EDX at magnification of: (a) 30X; (b) 500X.

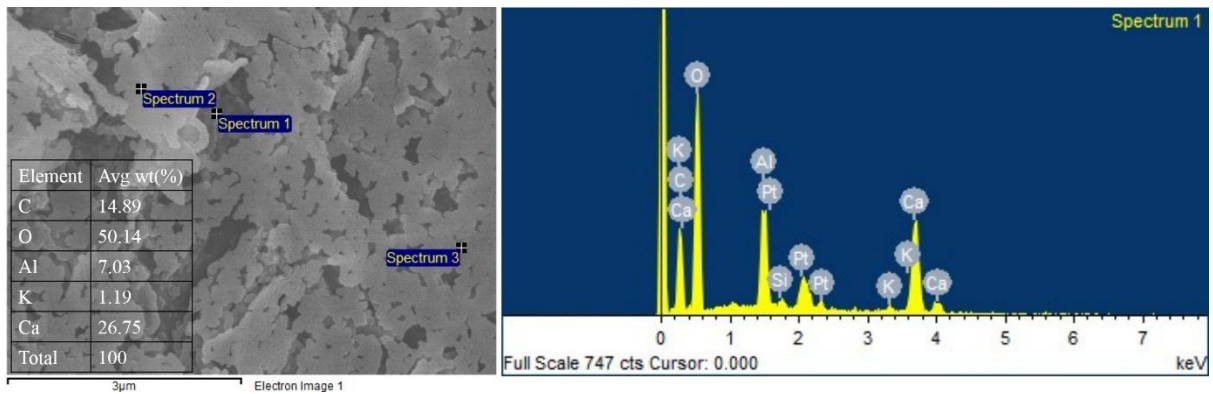


Figure 36: EDX analysis of precipitated crystals confirm presence of Ca element in all spectra (results are in weight % - only Spectrum 1 is shown).

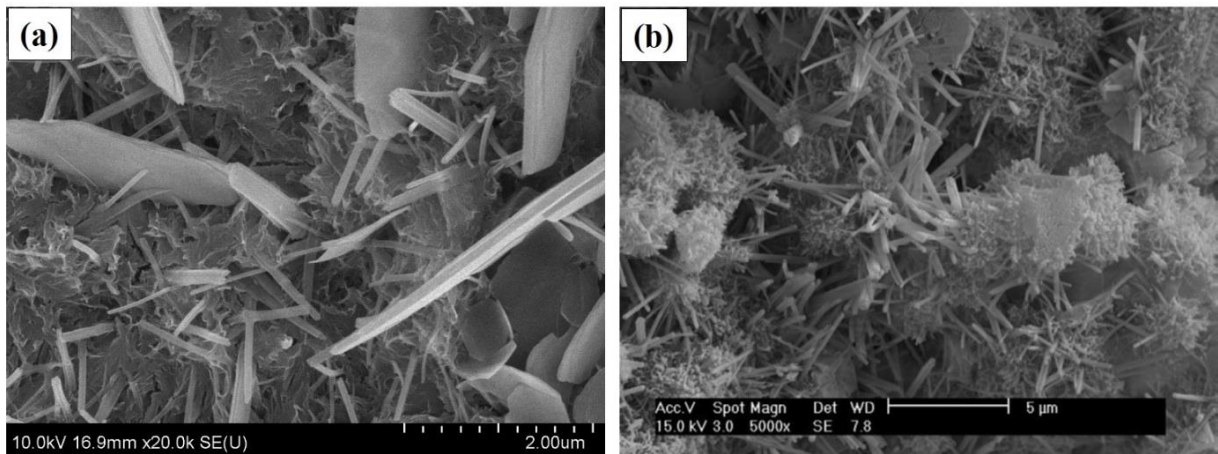


Figure 37: Ettringite crystals of cement paste: (a) control sample; (b) from literature [147].

**Thermogravimetric analysis** – TGA was conducted on the healed and the parent cement paste samples. Decomposition of  $\text{CaCO}_3$  to  $\text{CaO}$  and  $\text{CO}_2$  has occurred at a temperature range of 600-700° C [148]. As shown in Figure 38-a, decomposition of  $\text{CaCO}_3$  caused a weight loss in the healed cement paste, while the pure cement paste did not exhibit any weight loss within the same temperature range. It can be inferred that the healing products are calcium carbonate precipitated by bacteria through a metabolic conversion of the organic compound. The results confirm that healing product is  $\text{CaCO}_3$ .

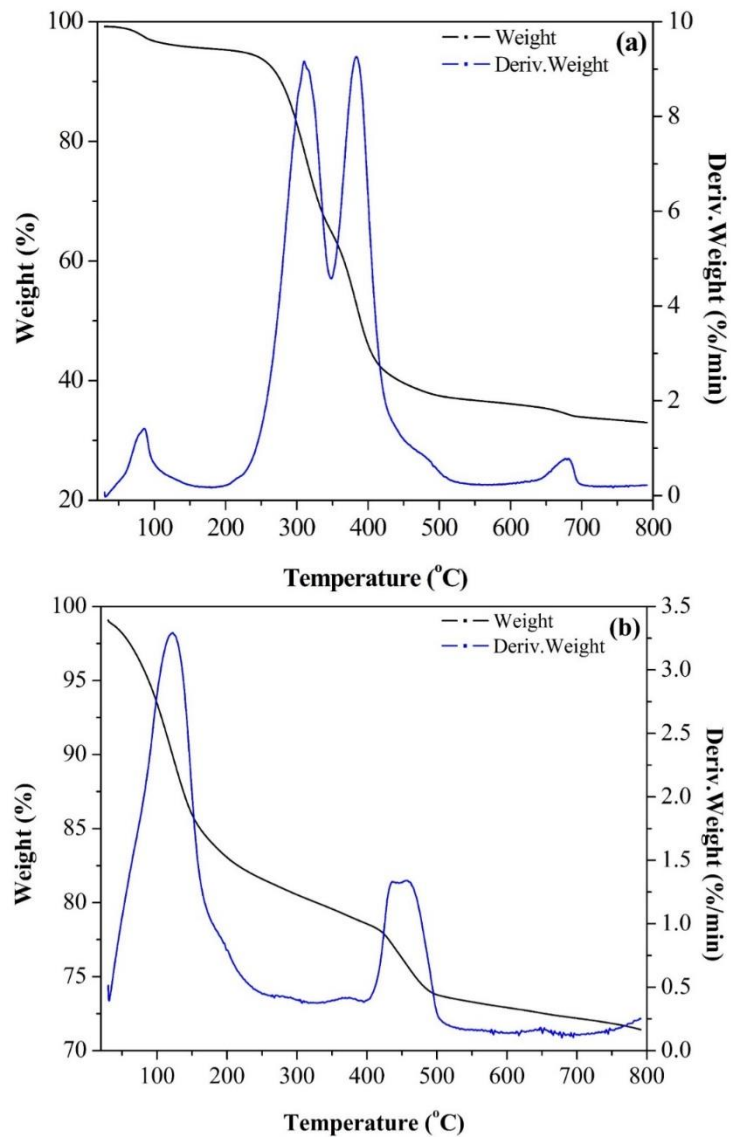


Figure 38: TGA graphs of the cement paste: (a) healed; (b) pure.

## 5. CONCLUSIONS

Bacterial based self-healing for cementitious materials is preferred over other approaches due to a number of advantages, such as environmental acceptability, non-toxicity, compatibility of produced calcium carbonate with the cement matrix, and longevity of bacterial spores. In this study, polyurea polymer was proposed as a new class of material for encapsulation of bacteria. As compared to the current self-healing carriers, polyurea polymer provides a fairly short curing time, longevity, adjustable brittleness and water insensibility. *Bacillus pstedofirmus* can successfully act as a healing agent. The spore sporulation of the bacteria was achieved using a standard method. Protection of the bacteria and nutrition is necessary to improve the healing efficiency. Therefore, in-situ polymerization method was employed for synthesis and encapsulation of the healing agent in polyurea capsules. The synthesized capsules were characterized using destructive and non-destructive testing methods. The results confirmed the presence of polyurea bonding, and most importantly the healing agent and nutrition were encapsulated. The presence of encapsulation has also shown no effect on the microcapsule structure.

This study has proven successful encapsulation of the bacterial spores and nutrition in polyurea through a series of destructive and non-destructive testing. It was concluded that upon rupturing, the capsuled bacterial spores are able to germinate from the dormant to active mode and consume the available nutrition to precipitate calcium carbonate needed for crack healing. The synthesized capsules were mixed with cement to confirm the occurrence of self-healing in an artificially cracked cement paste specimen. The precipitation of calcium carbonate was observed after 3 day. Morphology and chemical characterization of the materials from the healed crack confirmed the presence of calcium carbonate.

In summary, the study has shown that polyurea is a suitable shield with a high potential to protect bacteria and nutrition from the harsh environments in the cementitious matrix. This

capacity was observed during mixing with the cement paste and equally in the hardened form. Such conclusion positions polyurea as an excellent carrier that enables adequate bacterial viability and protection for self-healing in cementitious media.

## 6. CONSIDERATION FOR FUTURE STUDY

Optimization of the size and content of the polyurea capsules in a cement paste is not in the scope of the study. However, their incorporation in a cementitious matrix is expected to adversely affect its mechanical properties. As a pilot attempt to assess this effect, capsule contents of 1% and 3% (estimated as a percentage of the dry weight of cement) were considered. The capsules were mixed for 1 minute until homogenous dispersion was observed. Flexural strength test was applied to prismatic samples using the rectangular molds described in the experimental program. The compressive strength was also evaluated on 25mm cubes at a displacement rate of 0.5 mm/min. Three replicates of the flexural and compressive strengths of the specimens were measured after 7 and 28 day of curing (Table 9). The results indicate that the 28-day compressive strength of cement paste with 1% and 3% capsule content has been reduced by 3.5% and 15.6%, respectively, as compared to the control specimen. Similarly, the flexural strength of control sample was higher than those casted with self-healing capsules. In view of this, it is instrumental from the practical perspective to further investigate to what extent the inclusion of the polyurea capsules would penalize the strength versus the recovery that self-healing can bring. To this end, the optimum capsule content needed for feasible self-healing efficiency is recommended for future studies.

Table 9: Summarized Compressive and Flexural Strength Results for Samples

Sample	Avg. flex. strength- $\sigma$ (MPa)		Avg. comp. strength- $\sigma$ (MPa)	
	7 day	28 day	7 day	28 day
Control	8.30 (0.85)	9.50 (0.85)	45.51 (4.44)	58.88 (1.32)
1% Polyurea	6.20 (0.48)	6.68 (0.36)	46.97 (7.01)	56.83 (9.03)
3% Polyurea	6.17 (0.37)	7.11 (0.17)	33.35 (0.84)	49.71 (4.45)

$\sigma$  standard deviation

## References

1. Hassoun, M.N. and A. Al-Manaseer, *Structural concrete: theory and design*. 2012: John Wiley & Sons.
2. Koch, G., et al., *Corrosion costs and preventive strategies in the united states. report by cc technologies laboratories, inc. to federal highway administration (fhwa), office of infrastructure research and development*. Office of Infrastructure Research and Development. Report FHWA-RD-01-156, 2001.
3. Weiss, W.J., *Prediction of early-age shrinkage cracking in concrete elements*. 1999.
4. Schlangen, E. and C. Joseph, *Self-Healing Processes in Concrete*. Self-healing materials: Fundamentals, design strategies, and applications, 2009: p. 141-182.
5. Igarashi, S.-i., M. Kunieda, and T. Nishiwaki, *Technical committee on autogenous healing in cementitious materials*. Japan: JCI. TC075B, 2009.
6. De Rooij, M., et al., *Self-healing phenomena in cement-Based materials: state-of-the-art report of RILEM technical committee 221-SHC: self-Healing phenomena in cement-Based materials*. Vol. 11. 2013: Springer.
7. Van Tittelboom, K. and N. De Belie, *Self-healing in cementitious materials—A review*. *Materials*, 2013. **6**(6): p. 2182-2217.
8. Reinhardt, H.W.e.a., *Self-Healing Phenomena in Cement-Based Materials 65–117*. (Springer,2013).
9. Granger, S., et al., *Experimental characterization of the self-healing of cracks in an ultra high performance cementitious material: Mechanical tests and acoustic emission analysis*. *Cement and Concrete Research*, 2007. **37**(4): p. 519-527.
10. Parks, J., et al., *Effects of bulk water chemistry on autogenous healing of concrete*. *Journal of Materials in Civil Engineering*, 2010. **22**(5): p. 515-524.
11. Jacobsen, S., J. Marchand, and L. Boisvert, *Effect of cracking and healing on chloride transport in OPC concrete*. *Cement and Concrete Research*, 1996. **26**(6): p. 869-881.
12. Reinhardt, H.-W. and M. Jooss, *Permeability and self-healing of cracked concrete as a function of temperature and crack width*. *Cement and Concrete Research*, 2003. **33**(7): p. 981-985.
13. Jonkers, H.M., *Self Healing Materials (ed. Zwaag, P. S. van der)*. Springer Netherlands, 2007: p. 195-204.
14. Qian, S., J. Zhou, and E. Schlangen, *Influence of curing condition and precracking time on the self-healing behavior of engineered cementitious composites*. *Cement and concrete composites*, 2010. **32**(9): p. 686-693.
15. Dry, C., M. Corsaw, and E. Bayer, *A comparison of internal self-repair with resin injection in repair of concrete*. *Journal of adhesion science and technology*, 2003. **17**(1): p. 79-89.
16. Van Tittelboom, K., et al., *Self-healing efficiency of cementitious materials containing tubular capsules filled with healing agent*. *Cement and Concrete Composites*, 2011. **33**(4): p. 497-505.
17. Joseph, C., et al., *Experimental investigation of adhesive-based self-healing of cementitious materials*. *Magazine of Concrete Research*, 2010. **62**(11): p. 831-843.
18. Pelletier, M.M., et al., *Self-healing concrete with a microencapsulated healing agent*. *Cem. Concr. Res*, 2011.
19. Kishi, T., et al. *Self-healing behaviour by cementitious recrystallization of cracked concrete incorporating expansive agent*. in *Proceedings of the First International Conference on Self-healing Materials, 18-20 April*. 2007. Noordwijk aan Zee.
20. Sisomphon, K., O. Copuroglu, and E. Koenders, *Self-healing of surface cracks in mortars with expansive additive and crystalline additive*. *Cement and Concrete Composites*, 2012. **34**(4): p. 566-574.

21. Ahn, T.-H. and T. Kishi, *Crack self-healing behavior of cementitious composites incorporating various mineral admixtures*. Journal of Advanced Concrete Technology, 2010. **8**(2): p. 171-186.
22. Huang, H., et al., *Self-healing in cementitious materials: Materials, methods and service conditions*. Materials & Design, 2016. **92**: p. 499-511.
23. Sakai, K. *Recycling concrete, the present state and future perspective*. in *TCG-JSCE JOINT SEMINAR*. 2009.
24. Jonkers, H.M., et al., *Application of bacteria as self-healing agent for the development of sustainable concrete*. Ecological engineering, 2010. **36**(2): p. 230-235.
25. Sharma, T., et al., *Alkaliphilic Bacillus species show potential application in concrete crack repair by virtue of rapid spore production and germination then extracellular calcite formation*. Journal of Applied Microbiology, 2017. **122**(5): p. 1233-1244.
26. Han, N. and F. Xing. *Service life consideration of concrete structures in a broad perspective, keynote speech*. in *Proceedings, the 11th international symposium on structural engineering*. 2010.
27. Wang, J., et al., *Use of silica gel or polyurethane immobilized bacteria for self-healing concrete*. Construction and building materials, 2012. **26**(1): p. 532-540.
28. Wang, J., et al., *Self-healing concrete by use of microencapsulated bacterial spores*. Cement and Concrete Research, 2014. **56**: p. 139-152.
29. Edvardsen, C., *Water permeability and autogenous healing of cracks in concrete*. Materials Journal, 1999. **96**(4): p. 448-454.
30. Neville, A., *Autogenous healing—a concrete miracle?* Concrete international, 2002. **24**(11): p. 76-82.
31. Zwaag, S., *Self healing materials: an alternative approach to 20 centuries of materials science*. Vol. 30. 2008: Springer Science+ Business Media BV.
32. Ramm, W. and M. Biscopio, *Autogenous healing and reinforcement corrosion of water-penetrated separation cracks in reinforced concrete*. Nuclear Engineering and Design, 1998. **179**(2): p. 191-200.
33. Yang, Y., et al., *Autogenous healing of engineered cementitious composites under wet-dry cycles*. Cement and Concrete Research, 2009. **39**(5): p. 382-390.
34. Clear, C., *The effects of autogenous healing upon the leakage of water through cracks in concrete*. 1985.
35. Van Tittelboom, K., et al., *Influence of mix composition on the extent of autogenous crack healing by continued hydration or calcium carbonate formation*. Construction and Building Materials, 2012. **37**: p. 349-359.
36. Termkhajornkit, P., et al., *Self-healing ability of fly ash-cement systems*. Cement and Concrete Composites, 2009. **31**(3): p. 195-203.
37. Sahmaran, M., G. Yildirim, and T.K. Erdem, *Self-healing capability of cementitious composites incorporating different supplementary cementitious materials*. Cement and Concrete Composites, 2013. **35**(1): p. 89-101.
38. Huang, H., G. Ye, and D. Damidot, *Effect of blast furnace slag on self-healing of microcracks in cementitious materials*. Cement and concrete research, 2014. **60**: p. 68-82.
39. Boh, B. and B. Šumiga, *Microencapsulation technology and its applications in building construction materials Tehnologija mikrokapsuliranja in njena uporaba v gradbenih materialih*. RMZ—Materials and Geoenvironment, 2008. **55**(3): p. 329-344.
40. White, S.R., et al., *Autonomic healing of polymer composites*. Nature, 2001. **409**(6822): p. 794.
41. Dry, C., *Procedures developed for self-repair of polymer matrix composite materials*. Composite structures, 1996. **35**(3): p. 263-269.

42. Dry, C., *Three designs for the internal release of sealants, adhesives, and waterproofing chemicals into concrete to reduce permeability*. Cement and Concrete Research, 2000. **30**(12): p. 1969-1977.
43. Dry, C. and W. McMillan, *Three-part methylmethacrylate adhesive system as an internal delivery system for smart responsive concrete*. Smart Materials and Structures, 1996. **5**(3): p. 297.
44. Nishiwaki, T., H. Mihashi, and Y. Okuhara. *Fundamental study on self-repairing concrete using a selective heating device*. in *Sixth International Conference on Concrete under Severe Conditions: Environment and Loading* Centro de Investigacion y de Estudios Avanzados del IPN, Unidad Merida Consejo Nacional de Ciencia y Tecnologia, CONACyT Universidad Autonoma de Yucatan Gobierno del Estado de Yucatan H Ayuntamiento de la Ciudad de Merida H Ayuntamiento de la Ciudad de Progreso Asociacion Latinoamericana de Control de Calidad, Patologia y Recuperacion de la Construccion, ALCONPAT Mexico CEMEX Concretos SA de CV WR GRACE Holdings SA de CV PENMAR SA de CV SIKKA Mexicana SA de CV BASF Mexicana SA de CV. 2010.
45. Cailleux, E. and V. Pollet. *Investigations on the development of self-healing properties in protective coatings for concrete and repair mortars*. in *Proceedings of the 2nd International Conference on Self Healing Materials, Chicago, IL, USA*. 2009.
46. Sun, L., W.Y. Yu, and Q. Ge. *Experimental research on the self-healing performance of micro-cracks in concrete bridge*. in *Advanced Materials Research*. 2011. Trans Tech Publ.
47. Li, V.C., Y.M. Lim, and Y.-W. Chan, *Feasibility study of a passive smart self-healing cementitious composite*. Composites Part B: Engineering, 1998. **29**(6): p. 819-827.
48. Sisomphon, K., O. Copuroglu, and A. Fraaij, *Application of encapsulated lightweight aggregate impregnated with sodium monofluorophosphate as a self-healing agent in blast furnace slag mortar*. Heron, 56 (1/2), 2011.
49. Grieve, T.K.e.a., *TR22 Non-structural cracks in concrete* 2010.
50. Thao, T.D.P., et al., *Implementation of self-healing in concrete—Proof of concept*. The IES Journal Part A: Civil & Structural Engineering, 2009. **2**(2): p. 116-125.
51. Kaltzakorta, I.E., E. , *silica capsules encapsulating epoxy compounds for self-healing cementitious materials*. Proc. 3rd Int. Conf. Self Heal. Mater. Bath UK 2011.
52. Mihashi, H. and T. Nishiwaki, *Development of engineered self-healing and self-repairing concrete-state-of-the-art report*. Journal of Advanced Concrete Technology, 2012. **10**(5): p. 170-184.
53. Rodriguez-Navarro, C., et al., *Conservation of ornamental stone by Myxococcus xanthus-induced carbonate biomineralization*. Applied and Environmental Microbiology, 2003. **69**(4): p. 2182-2193.
54. De Muynck, W., et al., *Bacterial carbonate precipitation as an alternative surface treatment for concrete*. Construction and Building Materials, 2008. **22**(5): p. 875-885.
55. Jimenez-Lopez, C., et al., *Consolidation of quarry calcarenite by calcium carbonate precipitation induced by bacteria activated among the microbiota inhabiting the stone*. International Biodeterioration & Biodegradation, 2008. **62**(4): p. 352-363.
56. Le Metayer-Levrel, G., et al., *Applications of bacterial carbonatogenesis to the protection and regeneration of limestones in buildings and historic patrimony*. Sedimentary geology, 1999. **126**(1-4): p. 25-34.
57. Stocks-Fischer, S., J.K. Galinat, and S.S. Bang, *Microbiological precipitation of CaCO<sub>3</sub>*. Soil Biology and Biochemistry, 1999. **31**(11): p. 1563-1571.
58. Wiktor, V. and H.M. Jonkers, *Assessment of the crack healing capacity in bacteria-based self-healing concrete*. 2011.

59. Yang, Z., et al., *A self-healing cementitious composite using oil core/silica gel shell microcapsules*. Cement and Concrete Composites, 2011. **33**(4): p. 506-512.
60. Grantham, M., V. Mechtcherine, and U. Schneck, *Concrete Solutions 2011*. 2011: CRC Press.
61. *Autogenous Healing of Cement Paste*. ACI J. Proc. 52. 1956.
62. Tiano, P., et al., *Biomediated reinforcement of weathered calcareous stones*. Journal of Cultural Heritage, 2006. **7**(1): p. 49-55.
63. Ramakrishnan, V., et al. *4843-IMPROVEMENT OF CONCRETE DURABILITY BY BACTERIAL MINERAL PRECIPITATION*. in *ICF11, Italy 2005*. 2005.
64. Achal, V., et al., *Lactose mother liquor as an alternative nutrient source for microbial concrete production by Sporosarcina pasteurii*. Journal of industrial microbiology & biotechnology, 2009. **36**(3): p. 433-438.
65. Lark, R., A. Al-Tabbaa, and K. Paine, *Biomimetic multi-scale damage immunity for construction materials: M4L project overview*. 2013.
66. Mangat, P. and K. Gurusamy, *Permissible crack widths in steel fibre reinforced marine concrete*. Materials and structures, 1987. **20**(5): p. 338-347.
67. Van Tittelboom, K. and N. De Belie, *Self-healing concrete: suitability of different healing agents*. International Journal of 3R's, 2010. **1**(1): p. 12-21.
68. Mihashi, H., et al., *Fundamental study on development of intelligent concrete characterized by self-healing capability for strength*. Transactions of the Japan Concrete Institute, 2001. **22**: p. 441-450.
69. Xing, F., et al. *Self-healing mechanism of a novel cementitious composite using microcapsules*. in *Proceedings of the International Conference on Durability of Concrete Structures, Hangzhou, China*. 2008.
70. Van Tittelboom, K., et al., *Comparison of different approaches for self-healing concrete in a large-scale lab test*. Construction and building materials, 2016. **107**: p. 125-137.
71. Beglarigale, A., Y. Seki, and N.Y. Demir, *Sodium silicate/polyurethane microcapsules used for self-healing in cementitious materials: Monomer optimization, characterization, and fracture behavior*. Construction and Building Materials, 2018. **162**: p. 57-64.
72. Dong, B., et al., *Performance recovery concerning the permeability of concrete by means of a microcapsule based self-healing system*. Cement and Concrete Composites, 2017. **78**: p. 84-96.
73. Kanellopoulos, A., et al., *Polymeric microcapsules with switchable mechanical properties for self-healing concrete: synthesis, characterisation and proof of concept*. Smart Materials and Structures, 2017. **26**(4): p. 045025.
74. Kim, D.-M., et al., *Microcapsule-Type Self-Healing Protective Coating for Cementitious Composites with Secondary Crack Preventing Ability*. Materials, 2017. **10**(2): p. 114.
75. Li, W., et al., *Preparation and properties of melamine urea-formaldehyde microcapsules for self-healing of cementitious materials*. Materials, 2016. **9**(3): p. 152.
76. Jonkers, H.M., *Bacteria-based self-healing concrete*. Heron, 56 (1/2), 2011.
77. Wang, J., et al., *Application of hydrogel encapsulated carbonate precipitating bacteria for approaching a realistic self-healing in concrete*. Construction and building materials, 2014. **68**: p. 110-119.
78. Wang, J., N. De Belie, and W. Verstraete, *Diatomaceous earth as a protective vehicle for bacteria applied for self-healing concrete*. Journal of industrial microbiology & biotechnology, 2012. **39**(4): p. 567-577.

79. Gupta, S., H.W. Kua, and S. Dai Pang, *Healing cement mortar by immobilization of bacteria in biochar: An integrated approach of self-healing and carbon sequestration*. Cement and Concrete Composites, 2018. **86**: p. 238-254.
80. Bhaskar, S., et al., *Effect of self-healing on strength and durability of zeolite-immobilized bacterial cementitious mortar composites*. Cement and Concrete Composites, 2017. **82**: p. 23-33.
81. Seifan, M., et al., *Bio-reinforced self-healing concrete using magnetic iron oxide nanoparticles*. Applied microbiology and biotechnology, 2018. **102**(5): p. 2167-2178.
82. Sangadji, S. and E. Schlangen, *Self Healing of Concrete Structures-Novel approach using porous network concrete*. Journal of Advanced Concrete Technology, 2012. **10**(5): p. 185-194.
83. Sangadji, S. and E. Schlangen. *Porous network concrete: A new approach to make concrete structures self-healing using prefabricated porous layer*. in *Third international conference self-healing materials, Bath, United Kingdom*. 2011. Citeseer.
84. Nishiwaki, T., et al., *Development of self-healing system for concrete with selective heating around crack*. Journal of Advanced Concrete Technology, 2006. **4**(2): p. 267-275.
85. Nishiwaki, T., A. Oohira, and S. Pareek. *An experimental study on the application of self-repairing system to RC structures using selective heating*. in *Third international conference self-healing materials, Bath, United Kingdom*. 2011.
86. Kuang, Y.-c. and J.-p. Ou, *Passive smart self-repairing concrete beams by using shape memory alloy wires and fibers containing adhesives*. Journal of Central South University of Technology, 2008. **15**(3): p. 411-417.
87. De Muynck, W., N. De Belie, and W. Verstraete, *Microbial carbonate precipitation in construction materials: a review*. Ecological Engineering, 2010. **36**(2): p. 118-136.
88. Weiner, S. and P.M. Dove, *An overview of biomineralization processes and the problem of the vital effect*. Reviews in mineralogy and geochemistry, 2003. **54**(1): p. 1-29.
89. Frankel, R.B. and D.A. Bazylinski, *Biologically induced mineralization by bacteria*. Reviews in mineralogy and geochemistry, 2003. **54**(1): p. 95-114.
90. De Muynck, W., N. De Belie, and W. Verstraete. *Improvement of concrete durability with the aid of bacteria*. in *Proceedings of the first international conference on self healing materials*. 2007. Springer.
91. Ramachandran, S.K., V. Ramakrishnan, and S.S. Bang, *Remediation of concrete using micro-organisms*. ACI Materials Journal-American Concrete Institute, 2001. **98**(1): p. 3-9.
92. Day, J.L., V. Ramakrishnan, and S.S. Bang. *Microbiologically induced sealant for concrete crack remediation*. in *Proc. of 16th Engineering Mechanics Conference, Seattle*. 2003.
93. De Belie, N. and W. De Muynck. *Crack repair in concrete using biodeposition*. in *Proceedings of the International Conference on Concrete Repair, Rehabilitation and Retrofitting (ICRRR), Cape Town, South Africa*. 2008.
94. Ramakrishnan, V. *Performance characteristics of bacterial concrete—a smart biomaterial*. in *Proceedings of the First International Conference on Recent Advances in Concrete Technology*. 2007.
95. Bang, S., et al., *Microbial calcite, a bio-based smart nanomaterial in concrete remediation*. International Journal of Smart and Nano Materials, 2010. **1**(1): p. 28-39.

96. Achal, V., A. Mukherjee, and M.S. Reddy, *Effect of calcifying bacteria on permeation properties of concrete structures*. Journal of industrial microbiology & biotechnology, 2011. **38**(9): p. 1229-1234.
97. Richardson, A., K. Coventry, and J. Pasley, *Micro-induced Calcite Precipitation: Crack Sealing Application*. 2016.
98. Richardson, A., K. Coventry, and J. Pasley, *Bacterial crack sealing and surface finish application to concrete*. 2016.
99. Achal, V., A. Mukherjee, and M.S. Reddy, *Microbial concrete: way to enhance the durability of building structures*. Journal of materials in civil engineering, 2010. **23**(6): p. 730-734.
100. Ghosh, P., et al., *Use of microorganism to improve the strength of cement mortar*. Cement and Concrete Research, 2005. **35**(10): p. 1980-1983.
101. Jonkers, H.M. and E. Schlangen. *Crack repair by concrete-immobilized bacteria*. in *Proceedings of the first international conference on self healing materials*. 2007.
102. Wiktor, V. and H.M. Jonkers, *Quantification of crack-healing in novel bacteria-based self-healing concrete*. Cement and Concrete Composites, 2011. **33**(7): p. 763-770.
103. Wiktor, V. and H.M. Jonkers. *Self-healing of cracks in bacterial concrete*. in *2nd International Symposium on Service Life Design for Infrastructures*. 2010. RILEM Publications SARL.
104. Erşan, Y.Ç., et al., *Screening of bacteria and concrete compatible protection materials*. Construction and Building Materials, 2015. **88**: p. 196-203.
105. Zhang, J., et al., *Immobilizing bacteria in expanded perlite for the crack self-healing in concrete*. Construction and Building Materials, 2017. **148**: p. 610-617.
106. Soltmann, U., et al., *Biosorption of heavy metals by sol-gel immobilized Bacillus sphaericus cells, spores and S-layers*. Journal of sol-gel science and technology, 2003. **26**(1-3): p. 1209-1212.
107. Paine, K., *Bacteria-based self-healing concrete: Effects of environment, exposure and crack size*. 2016.
108. Dittrich, M., P. Kurz, and B. Wehrli, *The role of autotrophic picocyanobacteria in calcite precipitation in an oligotrophic lake*. Geomicrobiology Journal, 2004. **21**(1): p. 45-53.
109. Soltmann, U., B. Nies, and H. Böttcher, *Cements with embedded living microorganisms—a new class of biocatalytic composite materials for application in bioremediation, biotechnology*. Advanced Engineering Materials, 2011. **13**(1-2).
110. Achal, V., X. Pan, and N. Özyurt, *Improved strength and durability of fly ash-amended concrete by microbial calcite precipitation*. Ecological Engineering, 2011. **37**(4): p. 554-559.
111. Zhu, T., et al., *Potential application of biomineralization by Synechococcus PCC8806 for concrete restoration*. Ecological Engineering, 2015. **82**: p. 459-468.
112. Krumbein, W. and C. Giele, *Calcification in a coccoid cyanobacterium associated with the formation of desert stromatolites*. Sedimentology, 1979. **26**(4): p. 593-604.
113. De Belie, N., et al., *ICSHM 2013: Proceedings of the 4th International Conference on Self-Healing Materials, Ghent, Belgium, 16-20 June 2013*. 2013.
114. Sánchez-Ferrer, A., D. Rogez, and P. Martinoty, *Synthesis and characterization of new polyurea elastomers by sol/gel chemistry*. Macromolecular Chemistry and Physics, 2010. **211**(15): p. 1712-1721.
115. Tuerp, D. and B. Bruchmann, *Dendritic Polyurea Polymers*. Macromolecular rapid communications, 2015. **36**(2): p. 138-150.

116. Das, S., et al., *Structure–property relationships and melt rheology of segmented, non-chain extended polyureas: effect of soft segment molecular weight*. Polymer, 2007. **48**(1): p. 290-301.
117. Mattia, J. and P. Painter, *A Comparison of Hydrogen Bonding and Order in a Polyurethane and Poly (urethane– urea) and Their Blends with Poly (ethylene glycol)*. Macromolecules, 2007. **40**(5): p. 1546-1554.
118. Li, X.I. and D.j. Chen, *Synthesis and characterization of aromatic/aliphatic copolyureas*. Journal of applied polymer science, 2008. **109**(2): p. 897-902.
119. Pathak, J., et al., *Structure evolution in a polyurea segmented block copolymer because of mechanical deformation*. Macromolecules, 2008. **41**(20): p. 7543.
120. Fragiadakis, D., et al., *Segmental dynamics of polyurea: effect of stoichiometry*. Polymer, 2010. **51**(1): p. 178-184.
121. Wataru, S., *C. Koki anf T. Naoto*. J. Polym. Sci. Part B: Polym. Phys, 2001. **39**: p. 247.
122. Yilgor, I., et al., *Time-dependent morphology development in segmented polyetherurea copolymers based on aromatic diisocyanates*. Journal of Polymer Science Part B: Polymer Physics, 2009. **47**(5): p. 471-483.
123. Jewrajka, S.K., et al., *Polyisobutylene-based polyurethanes. II. Polyureas containing mixed PIB/PTMO soft segments*. Journal of Polymer Science Part A: Polymer Chemistry, 2009. **47**(11): p. 2787-2797.
124. Das, S., et al., *Probing the urea hard domain connectivity in segmented, non-chain extended polyureas using hydrogen-bond screening agents*. Polymer, 2008. **49**(1): p. 174-179.
125. Weathersby, P.K., T. Kolobow, and E.W. Stool, *Relative thrombogenicity of polydimethylsiloxane and silicone rubber constituents*. Journal of biomedical materials research, 1975. **9**(6): p. 561-568.
126. Hergenrother, R.W., Y. Xue-Hai, and S.L. Cooper, *Blood-contacting properties of polydimethylsiloxane polyureaurethanes*. Biomaterials, 1994. **15**(8): p. 635-640.
127. Son, H., et al., *Ureolytic/Non-ureolytic bacteria co-cultured self-healing agent for cementitious materials crack repair*. Materials, 2018. **11**(5): p. 782.
128. Sharma, K.S. and J. Sahoo, *Surfactant: Properties and applications*.
129. Kondo, T., *Microcapsules: their science and technology Part I. Various preparation methods*. Journal of oleo science, 2001. **50**(1): p. 1-11.
130. Alazhari, M., et al., *Application of expanded perlite encapsulated bacteria and growth media for self-healing concrete*. Construction and Building Materials, 2018. **160**: p. 610-619.
131. Arunkumar, T. and S. Ramachandran, *Surface coating and characterisation of polyurea for liquid storage*. International Journal of Ambient Energy, 2017. **38**(8): p. 781-787.
132. Sharma, Y., *Elementary Organic Spectroscopy, Principles and chemical applications*, S Chand & Co. Ltd, New Delhi, 2010: p. 89-150.
133. Cheong, S.H., *Physicochemical Properties of Calcium Lactate Prepared by Single-Phase Aragonite Precipitated Calcium Carbonate*. RESEARCH JOURNAL OF PHARMACEUTICAL BIOLOGICAL AND CHEMICAL SCIENCES, 2016. **7**(1): p. 1786-1794.
134. Rehman, F.-U.-. *Synthesis and Characterization of Speciality Polyurethane Elastomers 2010*: University Of Agriculture, Faisalabad. Pakistan
135. Williams, K. and S. Mason, *Future directions for Fourier Transform Raman spectroscopy in industrial analysis*. Spectrochimica Acta Part A: Molecular Spectroscopy, 1990. **46**(2): p. 187-196.

136. Kontoyannis, C.G. and N.V. Vagenas, *Calcium carbonate phase analysis using XRD and FT-Raman spectroscopy*. *Analyst*, 2000. **125**(2): p. 251-255.
137. Wagh, S., S. Dhumal, and A. Suresh, *An experimental study of polyurea membrane formation by interfacial polycondensation*. *Journal of Membrane Science*, 2009. **328**(1-2): p. 246-256.
138. Shang, J., et al., *A new route of CO<sub>2</sub> catalytic activation: syntheses of N-substituted carbamates from dialkyl carbonates and polyureas*. *Green Chemistry*, 2012. **14**(10): p. 2899-2906.
139. Wu, C., et al., *Polyureas from diamines and carbon dioxide: synthesis, structures and properties*. *Physical Chemistry Chemical Physics*, 2012. **14**(2): p. 464-468.
140. Hsieh, S.-C., et al., *A novel accelerator for improving the handling properties of dental filling materials*. *Journal of endodontics*, 2009. **35**(9): p. 1292-1295.
141. Vavrusova, M. and L.H. Skibsted, *Spontaneous supersaturation of calcium D-gluconate during isothermal dissolution of calcium L-lactate in aqueous sodium D-gluconate*. *Food & function*, 2014. **5**(1): p. 85-91.
142. Ni, M. and B.D. Ratner, *Differentiating calcium carbonate polymorphs by surface analysis techniques—an XPS and TOF-SIMS study*. *Surface and Interface Analysis: An International Journal devoted to the development and application of techniques for the analysis of surfaces, interfaces and thin films*, 2008. **40**(10): p. 1356-1361.
143. Palin, D., V. Wiktor, and H. Jonkers, *Bacteria-based self-healing concrete for application in the marine environment*. 2013.
144. Al-Jaroudi, S.S., et al., *Use of X-ray powder diffraction for quantitative analysis of carbonate rock reservoir samples*. *Powder Technology*, 2007. **175**(3): p. 115-121.
145. Khaliq, W. and M.B. Ehsan, *Crack healing in concrete using various bio influenced self-healing techniques*. *Construction and Building Materials*, 2016. **102**: p. 349-357.
146. Xu, J., W. Yao, and Z. Jiang, *Non-ureolytic bacterial carbonate precipitation as a surface treatment strategy on cementitious materials*. *Journal of Materials in Civil Engineering*, 2013. **26**(5): p. 983-991.
147. Artioli, G. and J.W. Bullard, *Cement hydration: the role of adsorption and crystal growth*. *Crystal Research and Technology*, 2013. **48**(10): p. 903-918.
148. Wang, J., et al. *Hydrogel encapsulated bacterial spores for self-healing concrete: Proof of concept*. in *4th International conference on Self-Healing Materials (ICSHM 2013)*. 2013. Ghent University. Magel Laboratory for Concrete Research.